The Abdus Salam
International Centre for Theoretical Physics

United Nations
Educational, Scientific and
Cultural Organization

IAEA
International Atomic Energy Agency

1936-13

Advanced School on Synchrotron and Free Electron Laser Sources and their Multidisciplinary Applications

7 - 25 April 2008

DEVELOPMENTS and APPLICATIONS of X-RAY MICROANALYTICAL TECHNIQUES BASED on X-RAY TUBES and SR SOURCES

Andrzej Markowicz
IAEA Laboratories
Seiberdforf

Austria

DEVELOPMENTS and APPLICATIONS of X-RAY MICROANALYTICAL TECHNIQUES BASED on X-RAY TUBES and SR SOURCES

Andrzej Markowicz

IAEA Laboratories
Seibersdorf
Austria

IAEA
International Atomic Energy Agency

ICTP, Trieste, 22 April 2008

Outline

1. Introduction
2. Micro-analytical techniques
3. Selected applications
4. Micro-tomography
5. Confocal setup
6. Sample preparation procedures
7. SR-based applications
8. Training
9. Conclusions

1. Introduction

- Assistance in establishing a modern and safe technological base to implement nuclear techniques and technologies for peaceful applications
- Laboratories at Seibersdorf and Monaco provide experimental support to the Agency's programmes
- Transfer of technologies through Technical Co-operation (TC)

1. IAEA Seibersdorf Laboratories

The IAEA Laboratories are located about 35 km south of Vienna, Austria

IAEA

1. Introduction (cont.)

XRF Laboratory at Seibersdorf

- R & D
- Analytical services
- Co-ordination and support of research
- Proficiency tests
- Development of QA/QC procedures
- Technical backstopping to TC projects
- Training
- Dissemination of information

2. Facilities and techniques available

Laboratory instruments and techniques

- EDXRF spectrometers
- Total reflection XRF spectrometers
- Micro-beam X-ray fluorescence and absorption technique

2. Secondary, polarizing target spectrometers

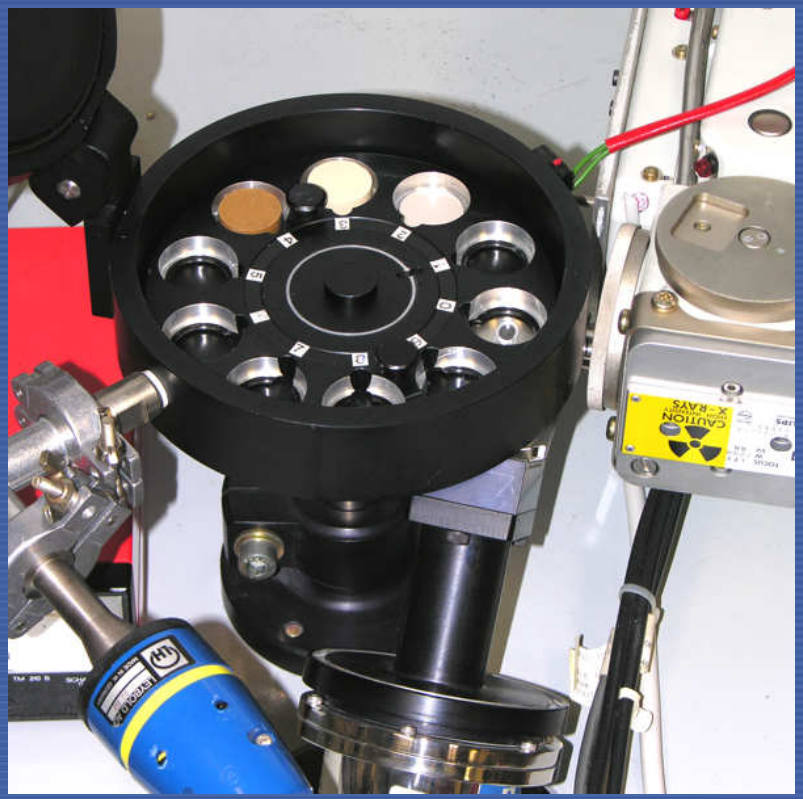

Left: heavy-duty, fully software controlled EDXRF spectrometer (Pd-anode X-ray tube) utilizing 5 secondary targets (Pd, HOPG, Co, Mo, Al_2O_3); right: in-house assembled EDXRF spectrometer (Cr-, Fe-, Cu-, Mo-, Rh-, Ag-, W-anode), manual selection of secondary targets (Mo, Rh, Ti in use, any other solid target possible)

2. Comparison of X-ray spectra

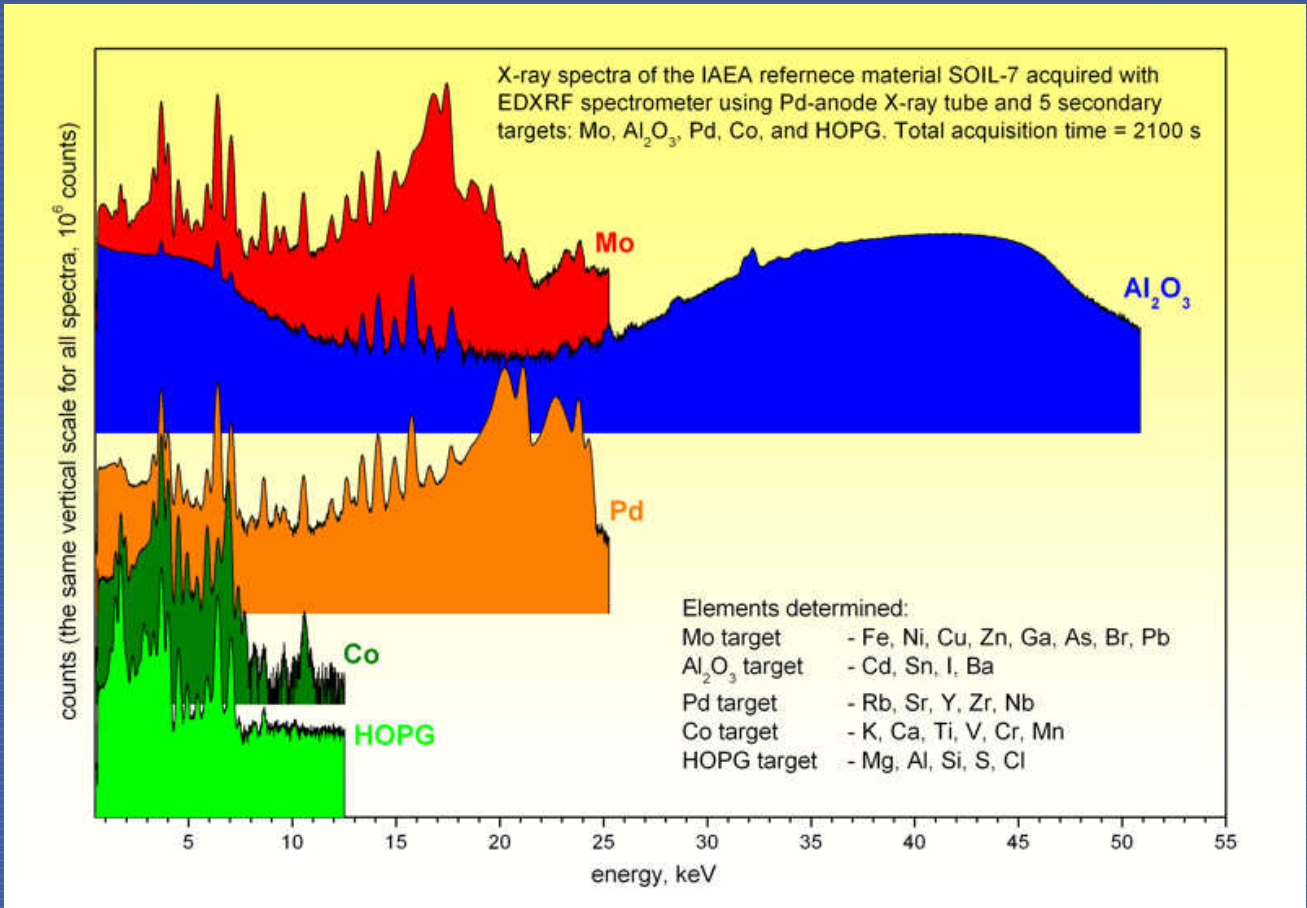

X-ray spectra of a “thick” pellet sample made of Soil-7 reference material excited in the EDXRF secondary target spectrometer.

IAEA

2. Total reflection X-ray fluorescence spectrometers

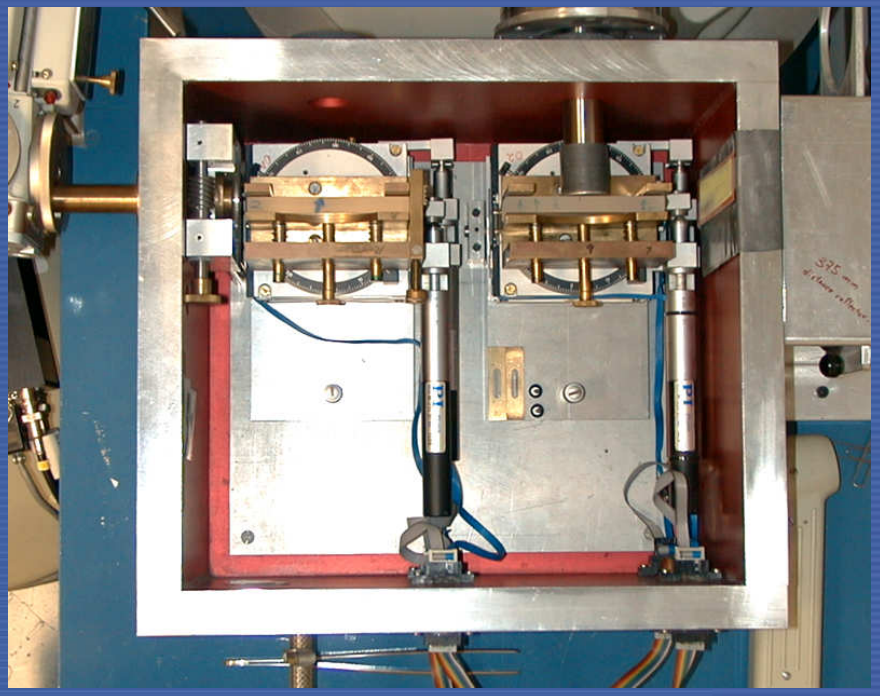

TXRF spectrometers, left: with 12-position sample changer; right: with motorized beam modifier and sample reflector stages

2. Micro-beam X-ray Setup Scheme

spatial resolution:

15 - 40 μm

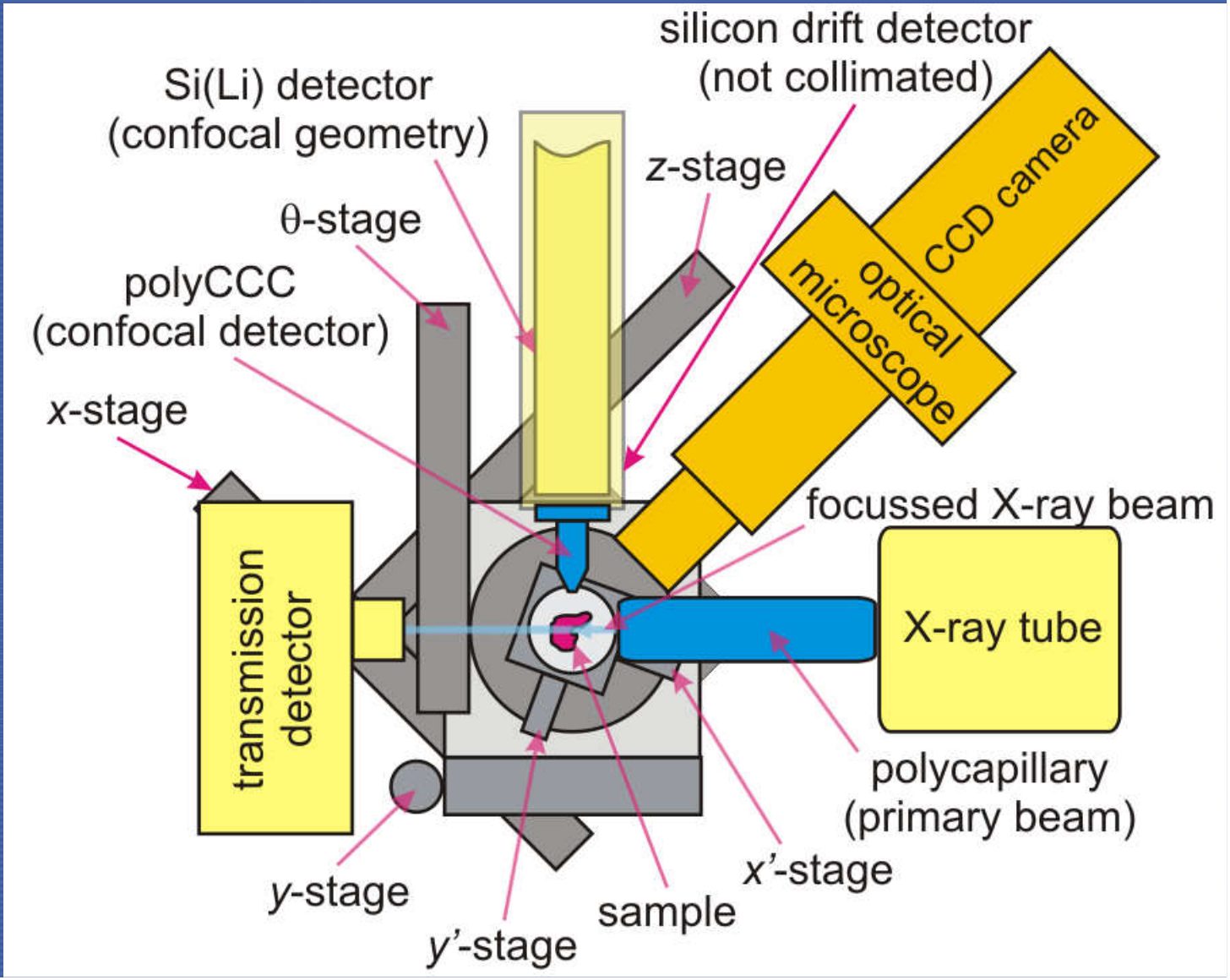

IAEA

2.The Micro-Beam X-ray Scanning Spectrometer

Si drift detector (fluorescence) on a stage

optical microscope

X-ray tube

Si(Li) detector (confocal)

transmission detector stage

sample stage

optical bench

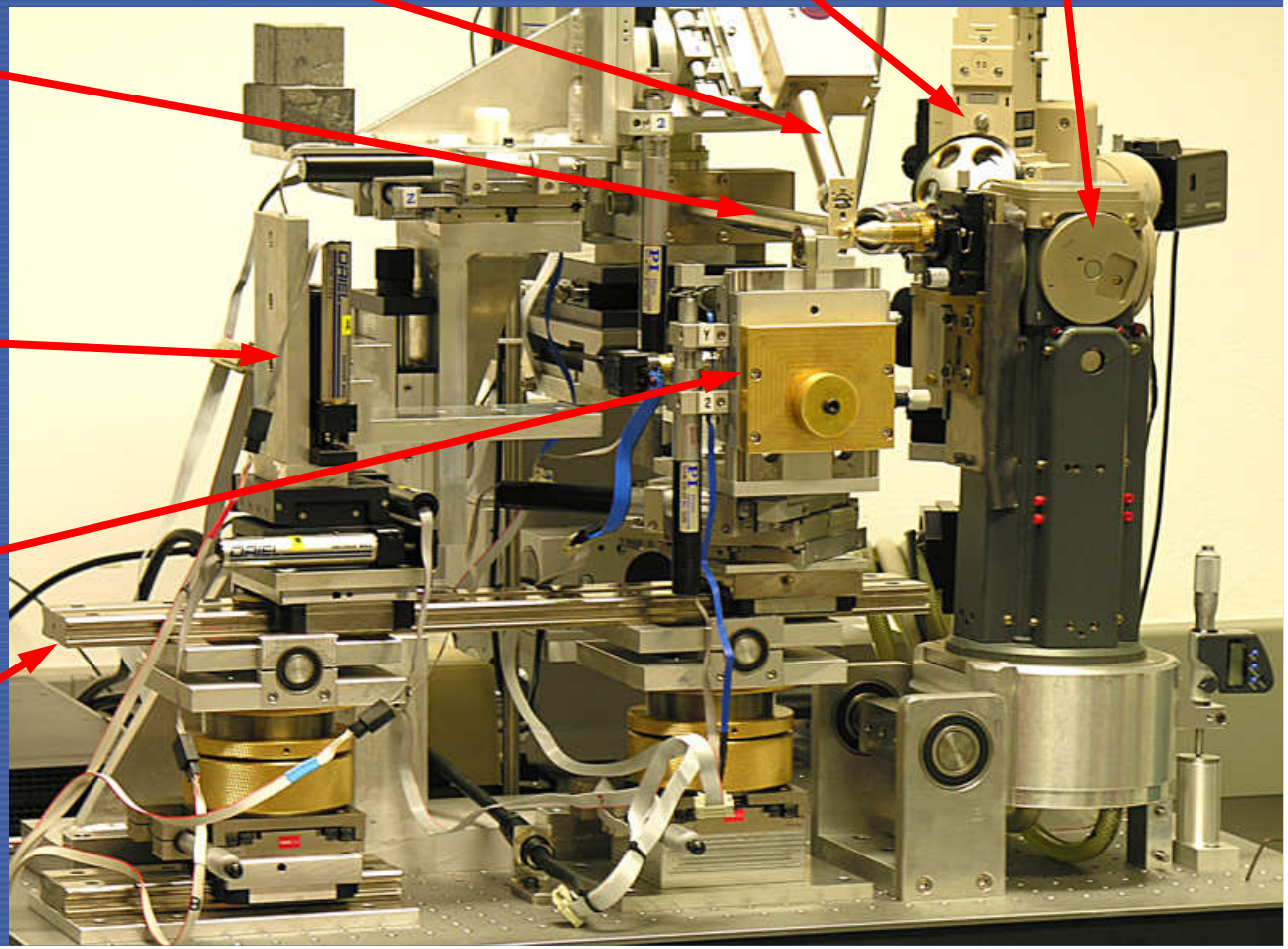

IAEA

2. Measuring geometry

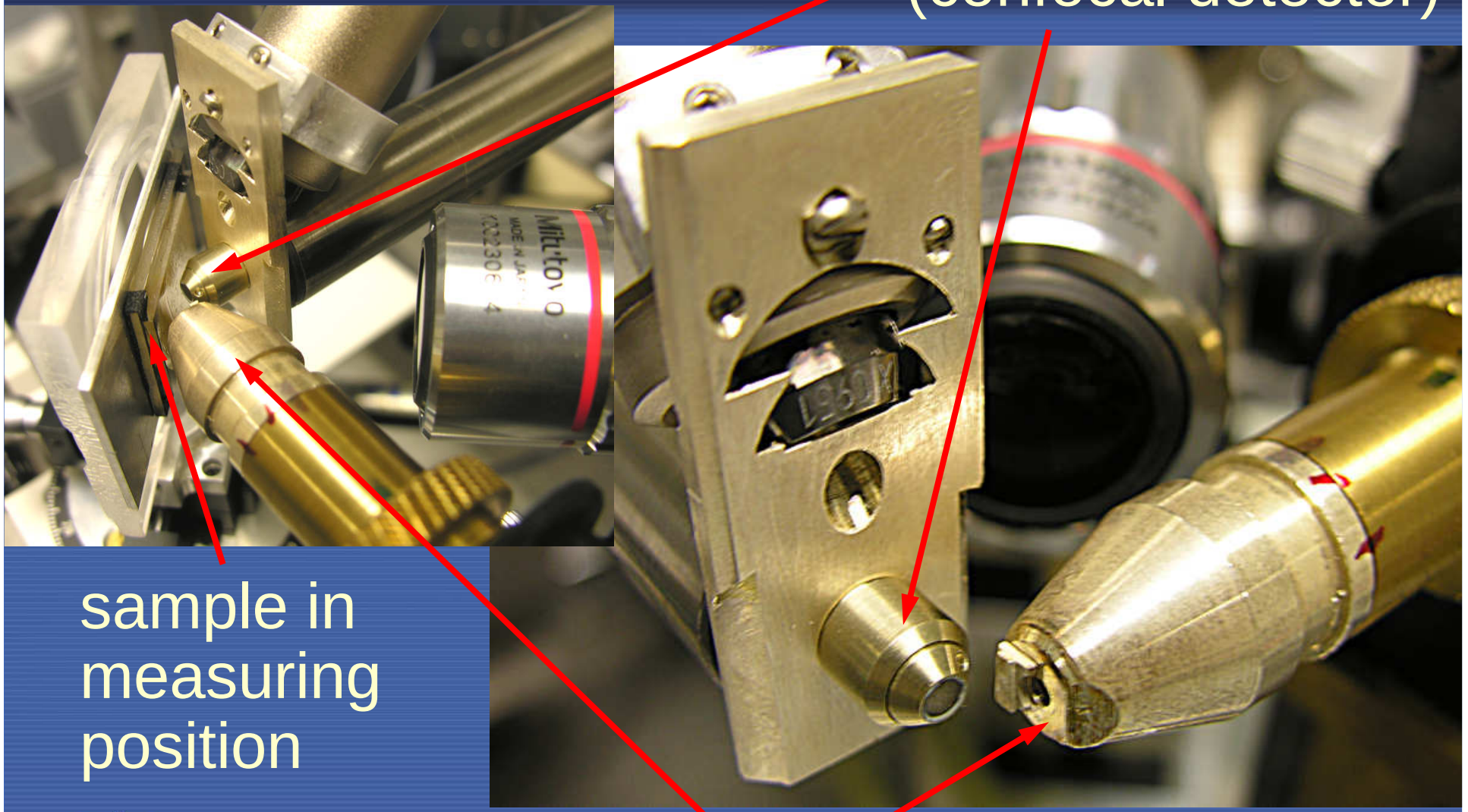

2. Detection Limits of Elements

40 μm
t = 1000s

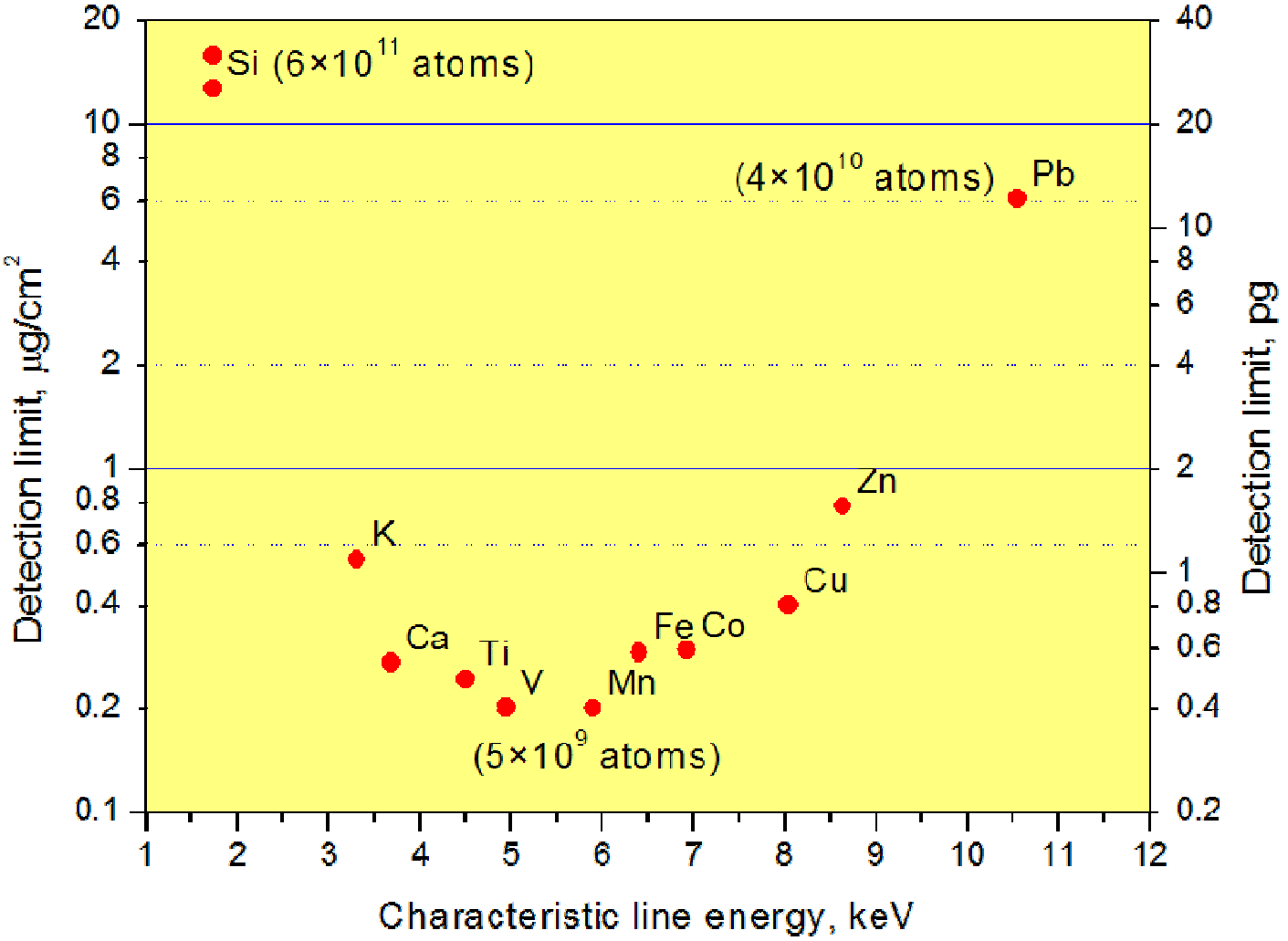

IAEA

2. Data acquisition software

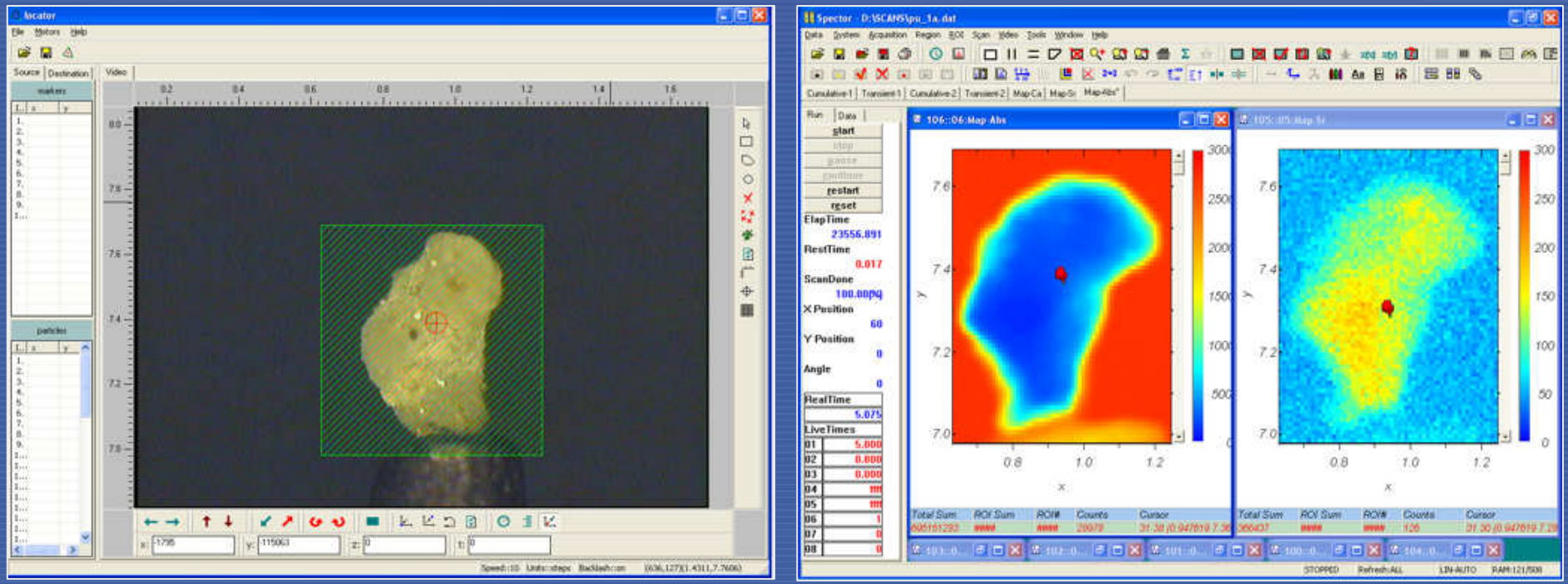

SPECTOR-LOCATOR: microscopic image of the sample (×150) and the collected X-ray absorption/fluorescence images

3. Detection of U-rich particles in contaminated soil

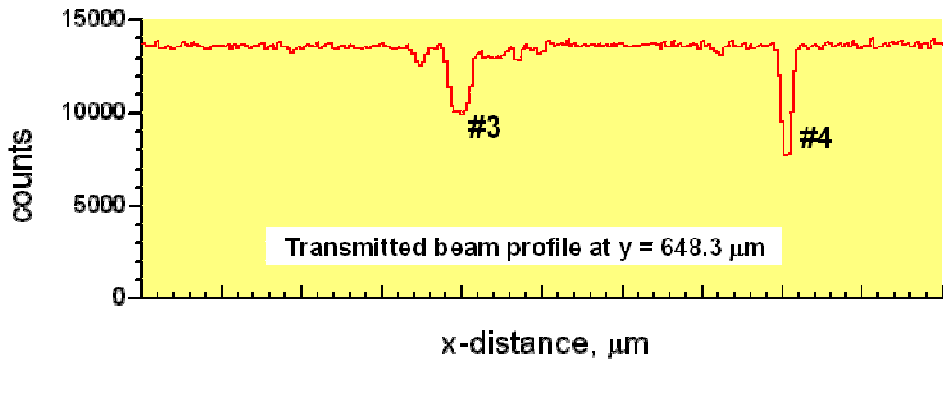

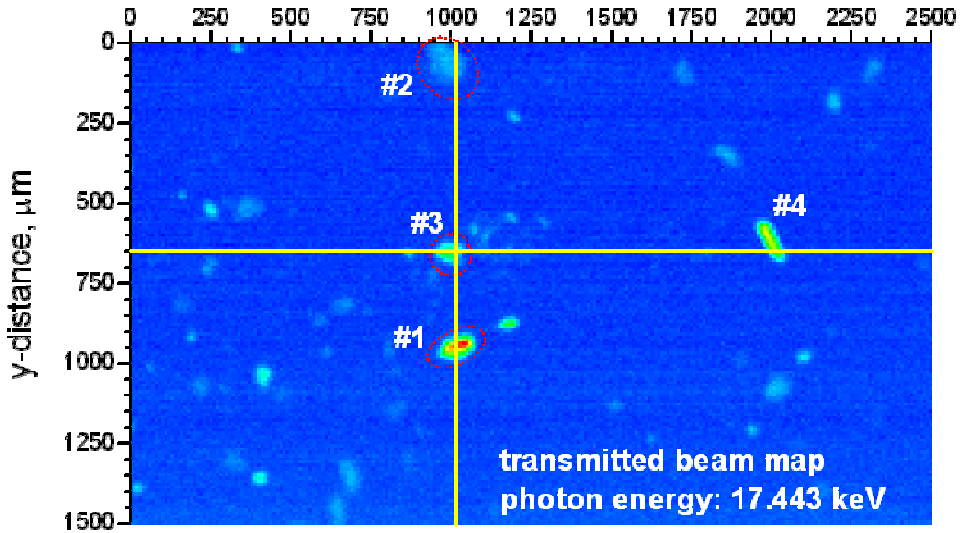

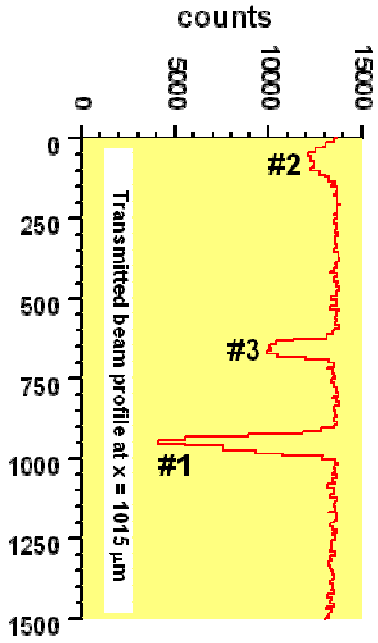

3. Detection of U-rich particles in contaminated soil

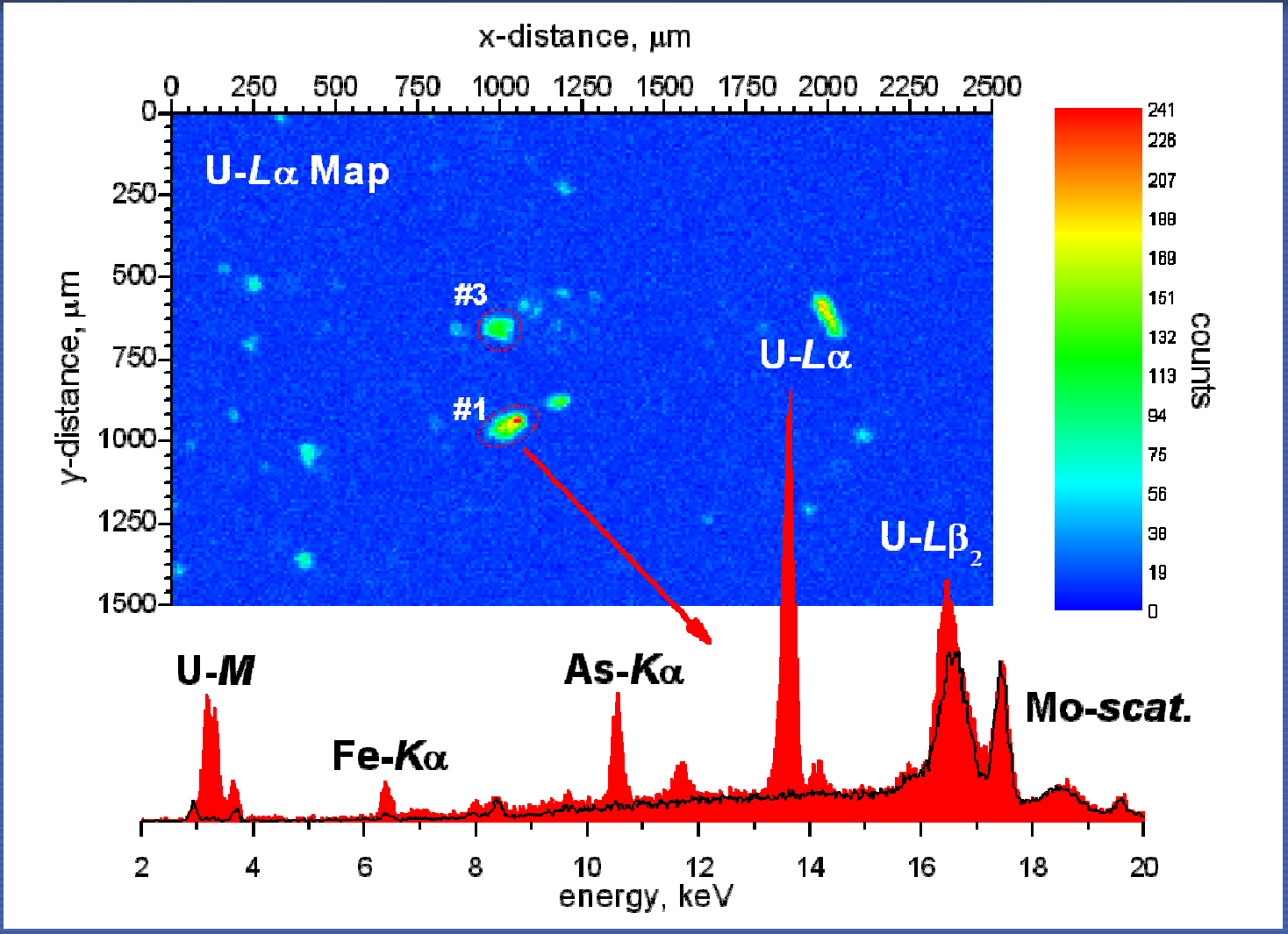

3. Detection of U-rich particles in contaminated soil

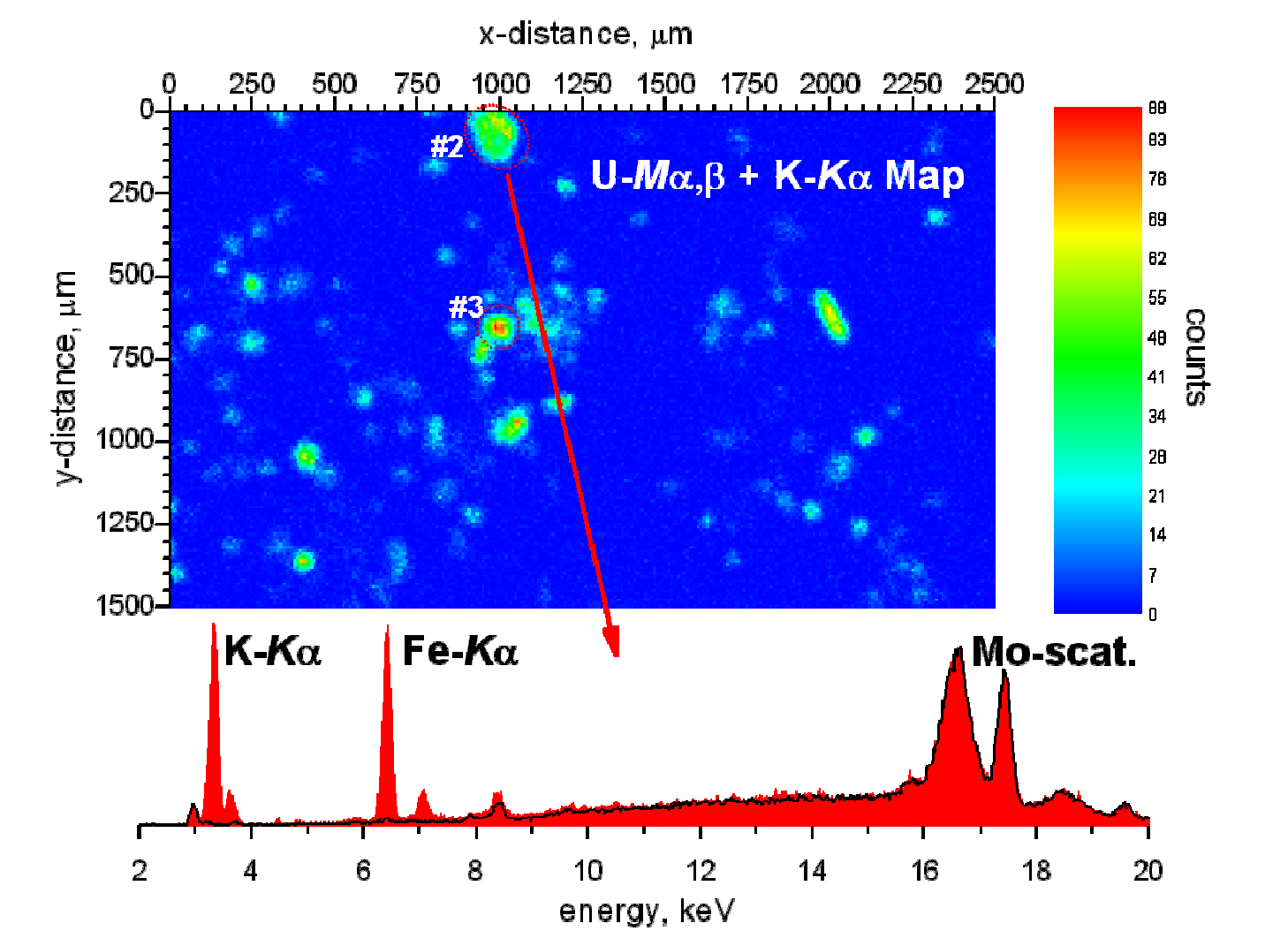

3. Detection of U-rich particles in contaminated soil

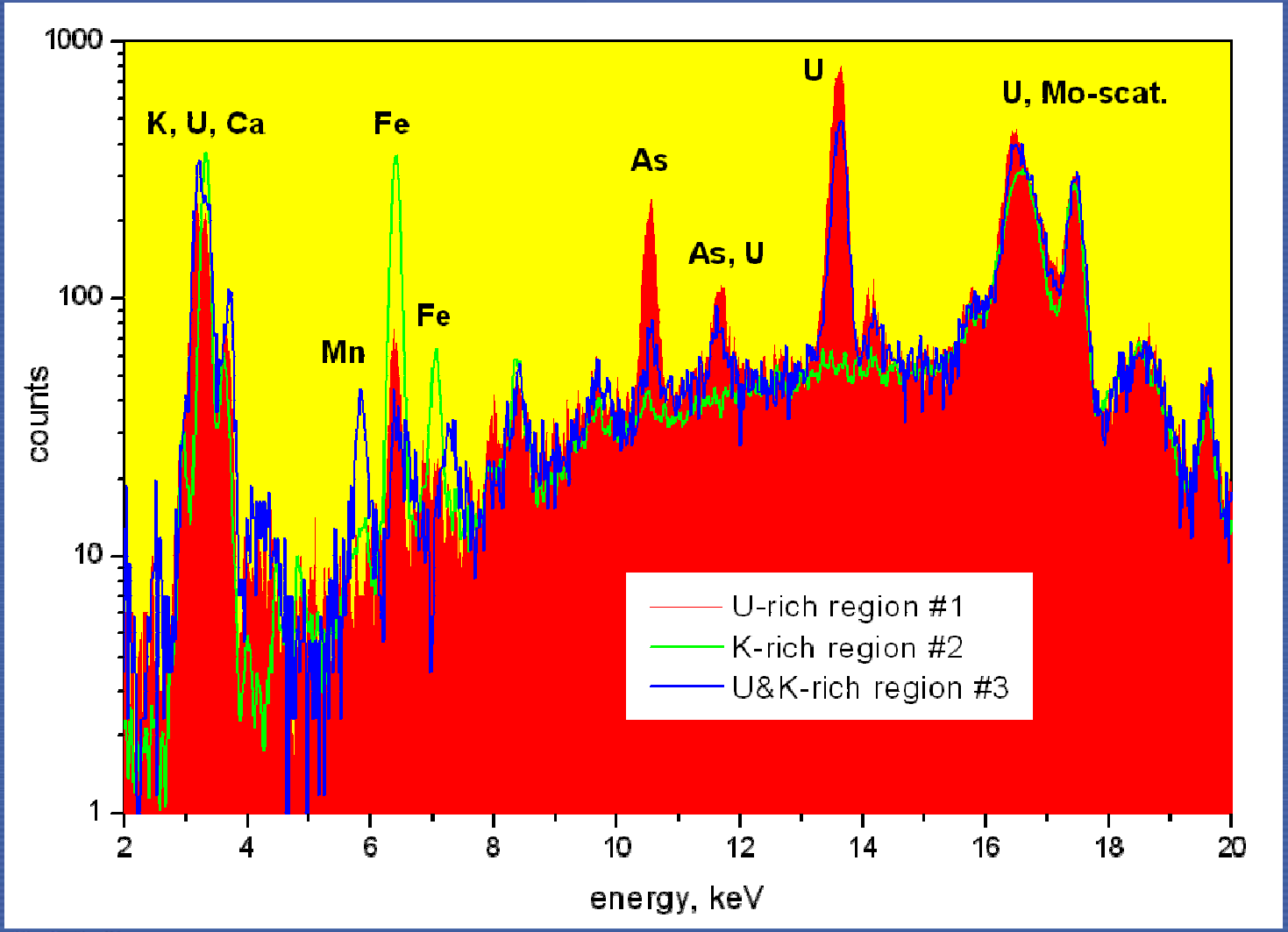

3. Identification of minerals

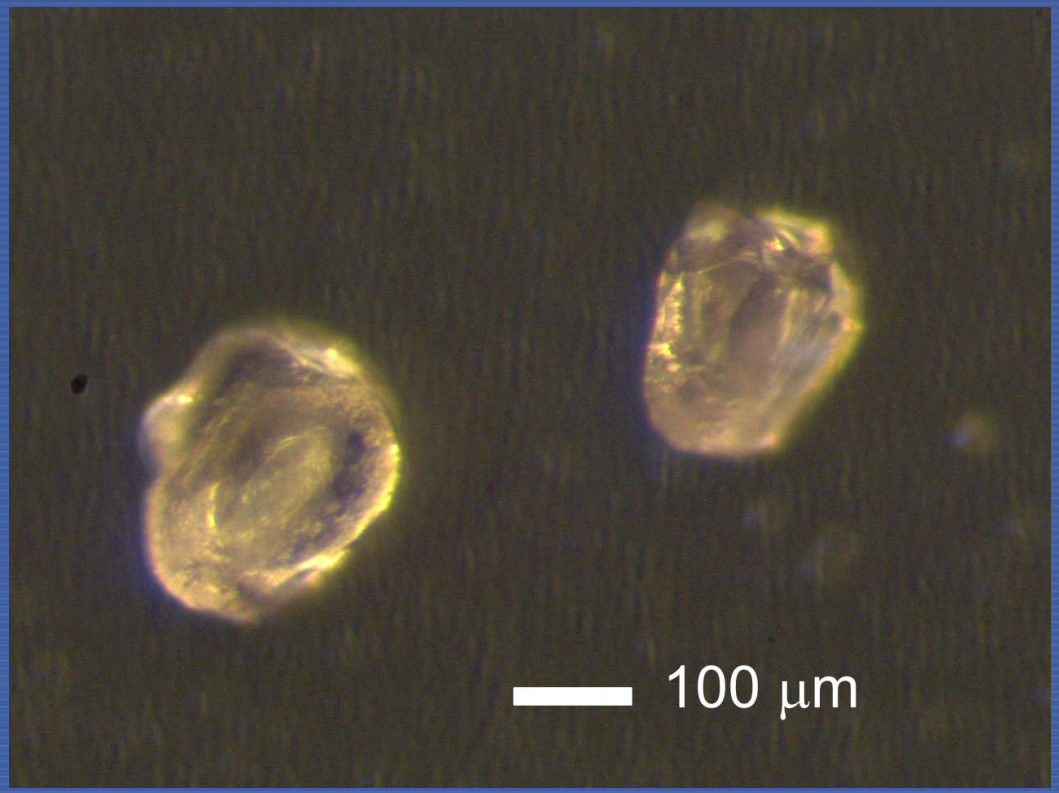

Two “similar” garnets: almandine-spessartine (left) and almandine (right)

3. Identification of minerals

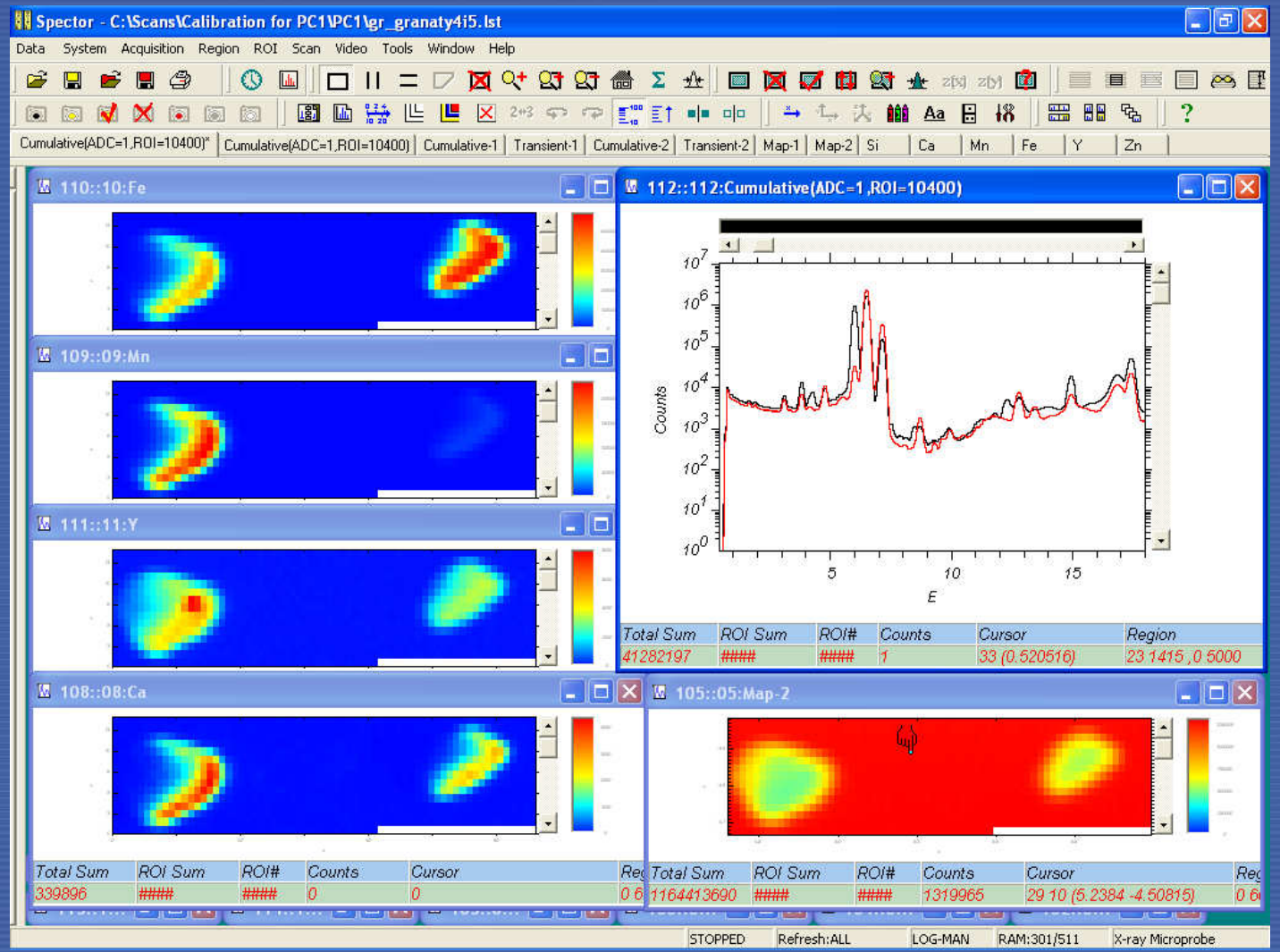

3. Homogeneity testing of a candidate Reference Material

- Based of the cumulative X-ray fluorescence spectrum of the MERCK CertiPUR standard the sensitivity curve is established. The thickness of the standard residue, confirmed by the data from transmission measurements, was well within the “thin sample” approximation – the sensitivity values were calculated assuming a “thin sample” model.

- The sensitivities obtained in step 1 are used to calculate the element concentrations in the dried residue samples prepared from the candidate RM. The obtained concentrations are corrected for absorption, using the data from transmission measurements.

3. Homogeneity testing of a candidate Reference Material

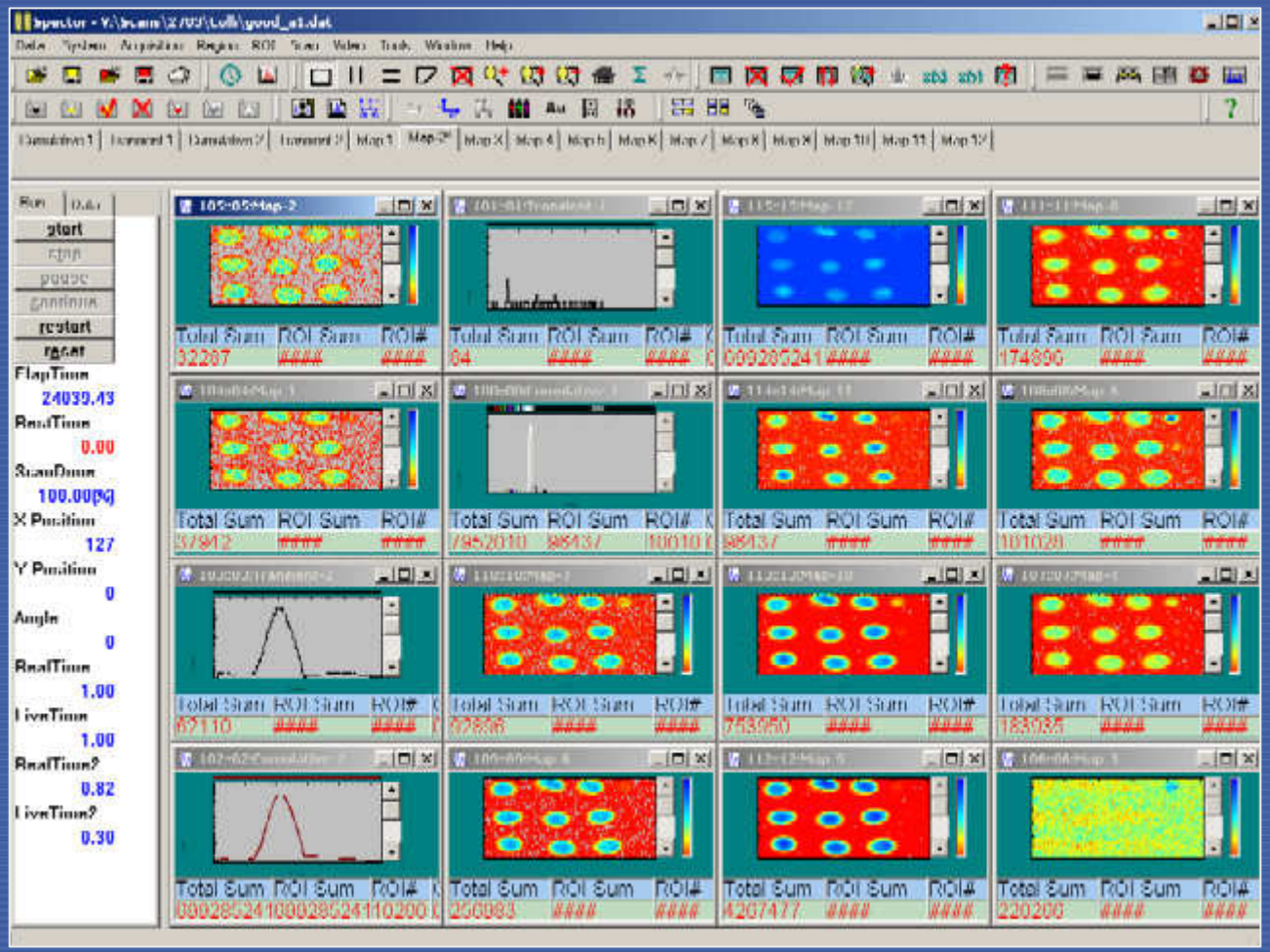

3. Homogeneity testing of a candidate Reference Material

- Determination of the sensitivity calibration curve:

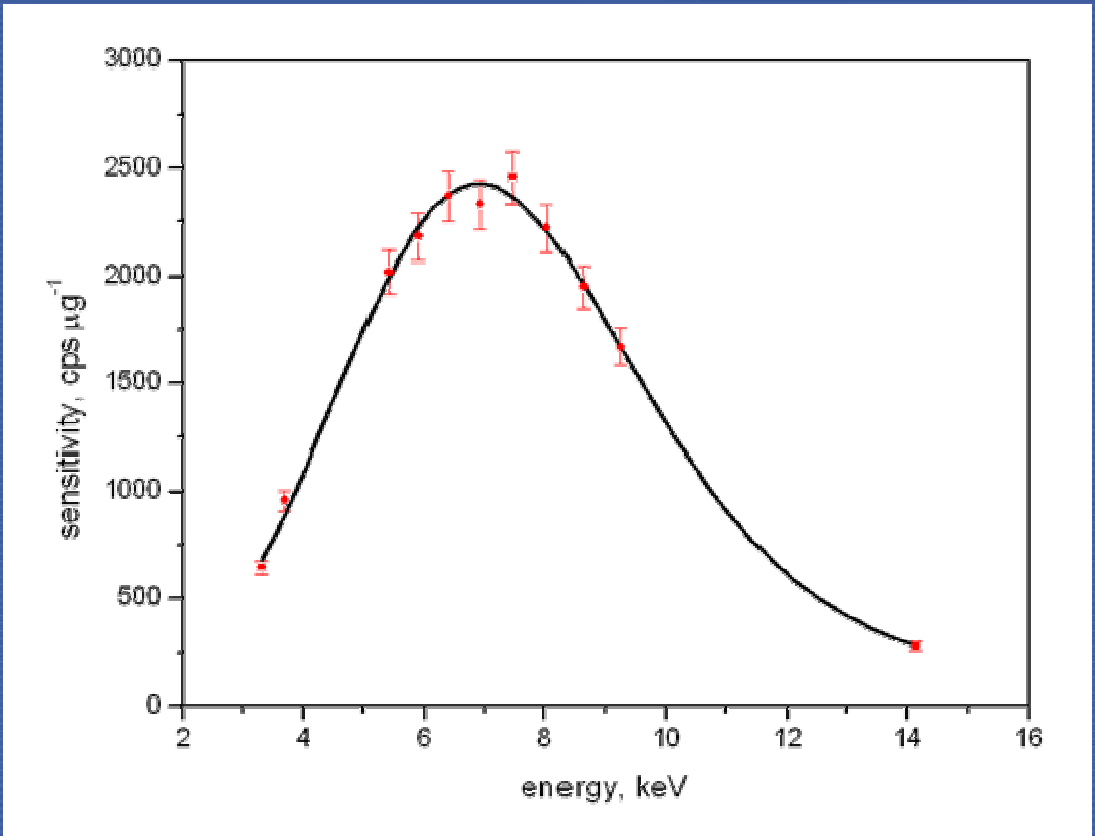

$$(I)_S = S(Z)m$$

$$(I)_x \approx S(Z_x)m_x F(E_{eff}, E_x)$$

$$c_x = \frac{m_x}{m_u}$$

3. Homogeneity testing of a candidate Reference Material

$$F(E_{eff}, E_x) = \frac{1 - \exp\{-((\mu\rho d)_{eff} + (\mu\rho d)_x)\}}{(\mu\rho d)_{eff} + (\mu\rho d)_x}$$

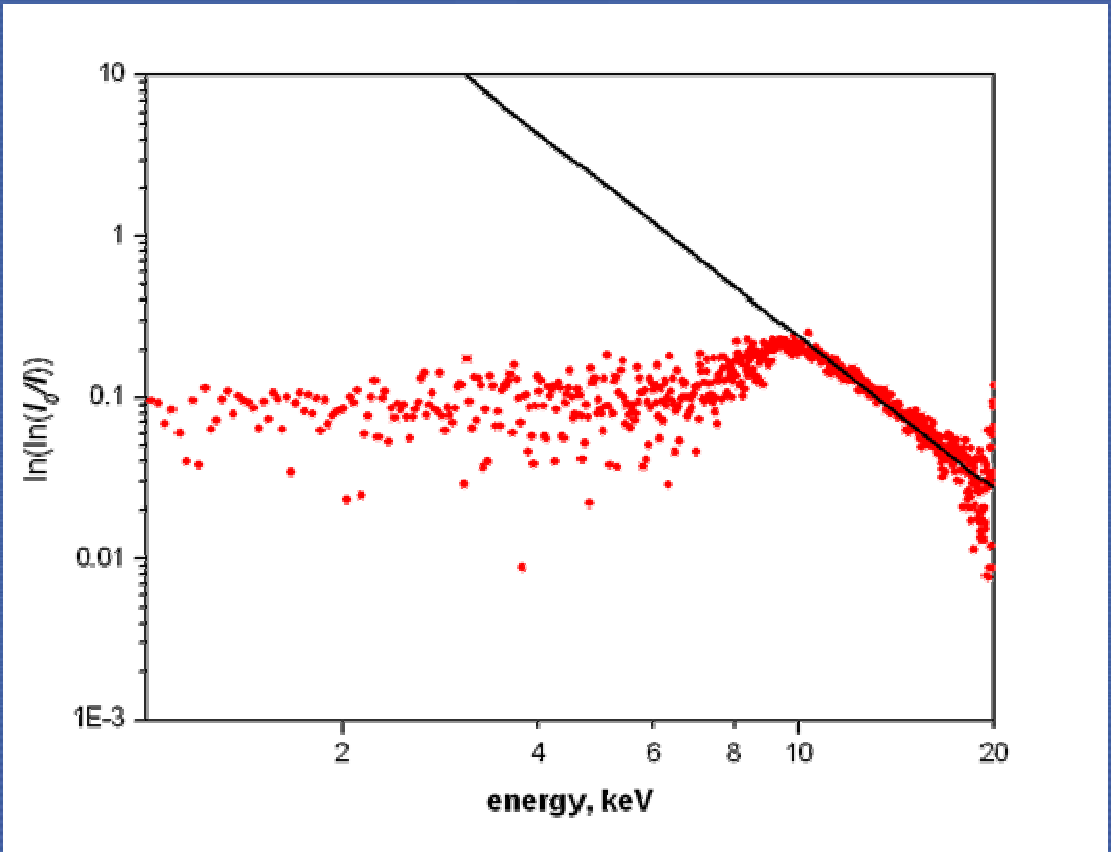

- Estimation of the absorption correction factor

3. Homogeneity testing of a candidate Reference Material

	Known Concentration	Determined Concentration
Ti	0.884% (0.082)	0.82 % (0.055)
Cr	352 ppm (22)	288 ppm (50)
Mn	1757 ppm (58)	1670 ppm (90)
Fe	7.91 % (0.24)	6.8 % (0.3)

4. CT Principle – Parallel Beam Projections

2D/3D CT scan (absorption and/or fluorescence)

Absorption correction of the fluorescence sinograms

Construction of interpolated sinograms for 3D scans

Reconstruction of the object cross-section(s) by filtered back projection algorithm

Volumetric rendering, 3D reconstruction, 3D mapping of element distribution, volume and area measurements

4. CT Principle – Parallel Beam Projections

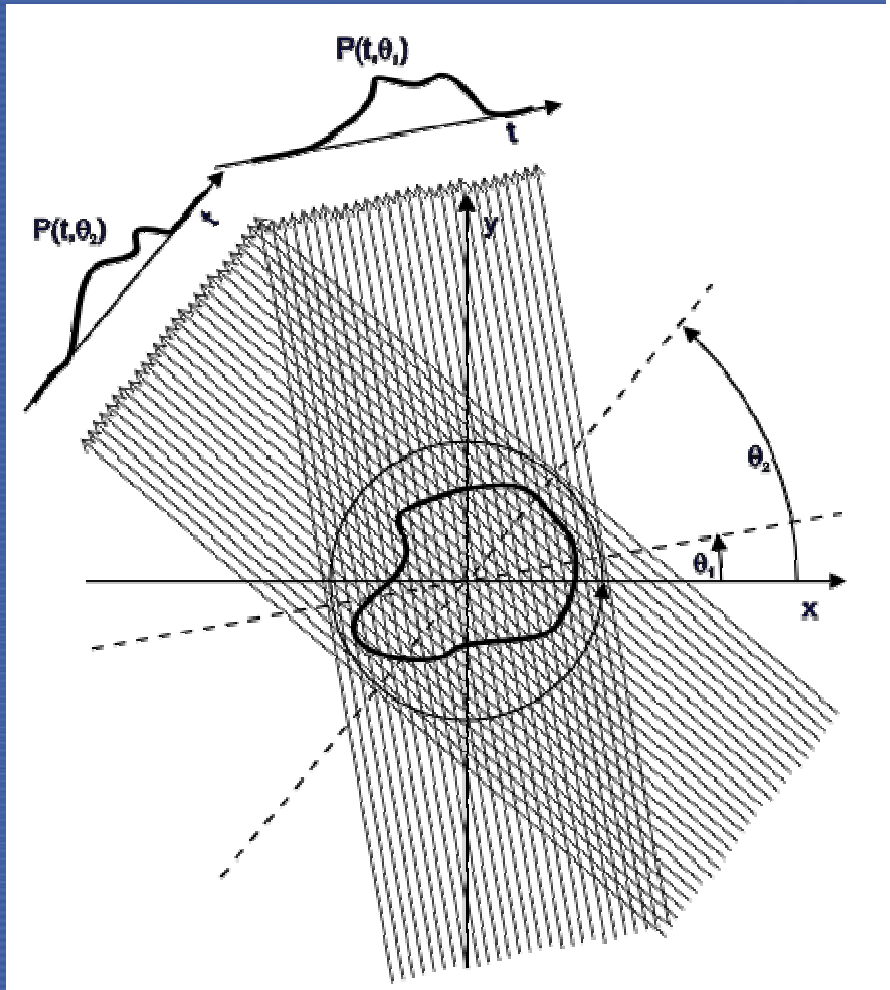

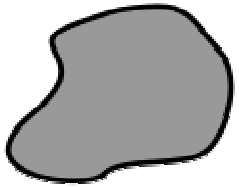

$$I(\theta,t) = I_0 e^{-\int_0^{l_{\theta,t}} \mu(x,y)\,dl}$$

$$P(\theta,t) = \ln\frac{I_0}{I(\theta,t)} = \int_0^{l_{\theta,t}} \mu(x,y)\,dl$$

$$Q(\theta,n\tau) = \tau \times IFFT\left\{\left[FFT\left(P(\theta,n\tau)\right)\right] \times \left[FFT\left(Filter(n\tau)\right)\right]\right\}$$

$$\mu(x,y) = \frac{\pi}{m}\sum_{i=1}^{m} Q(\theta_i, x\cos\theta_i + y\sin\theta_i)$$

IAEA

4. CT Absorption and XRF Imaging

Simultaneous X-ray absorption and X-ray fluorescence imaging in a “pencil” beam geometry

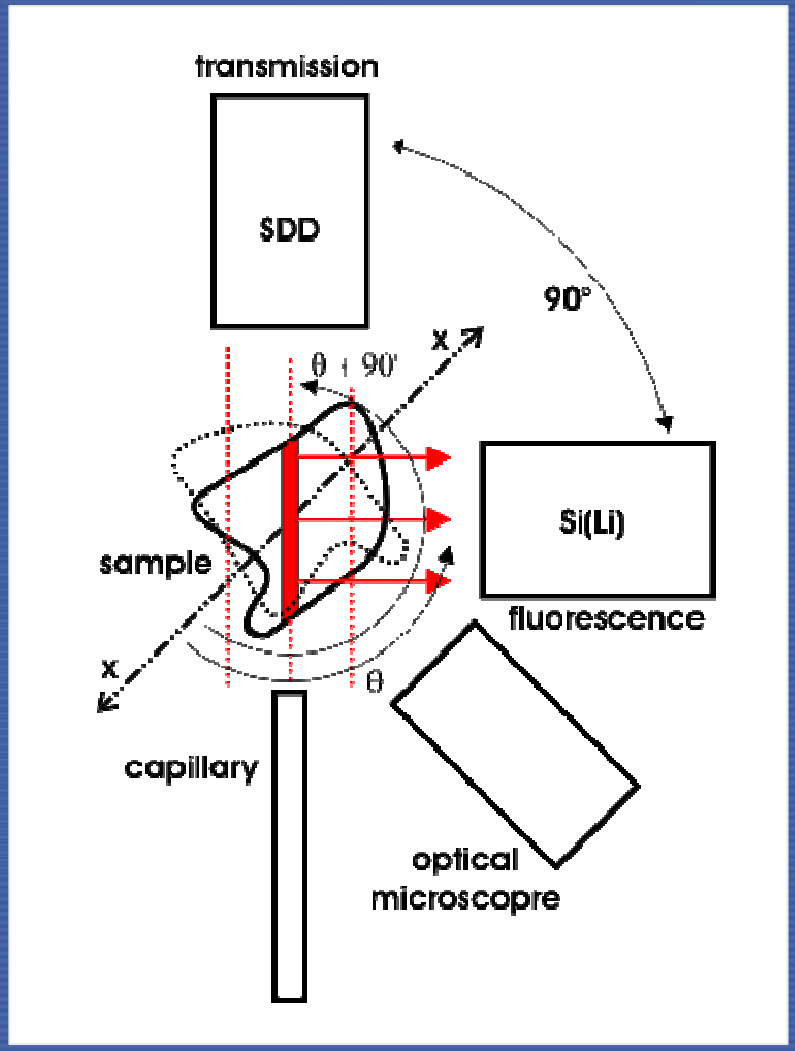

4. CT Absorption and XRF Imaging

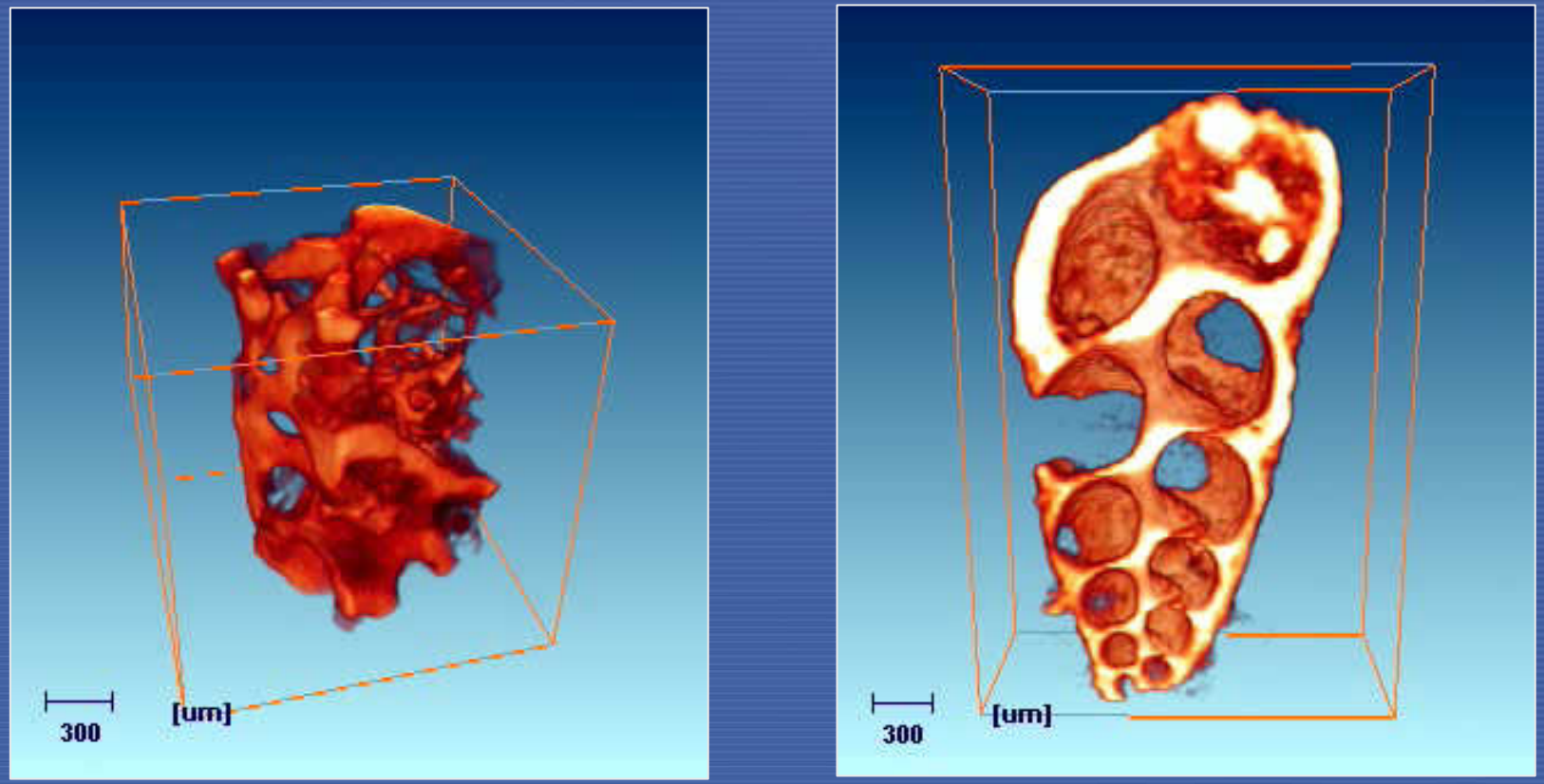

Reconstructed volumetric models of an osteoporotic bone fragment (left) and a shell fossil (right). CT absorption scan mode.

4. Depleted Uranium Particle

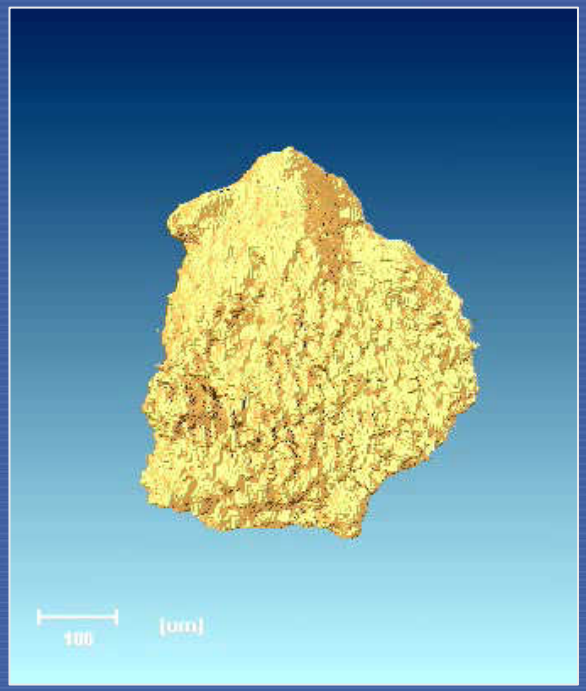

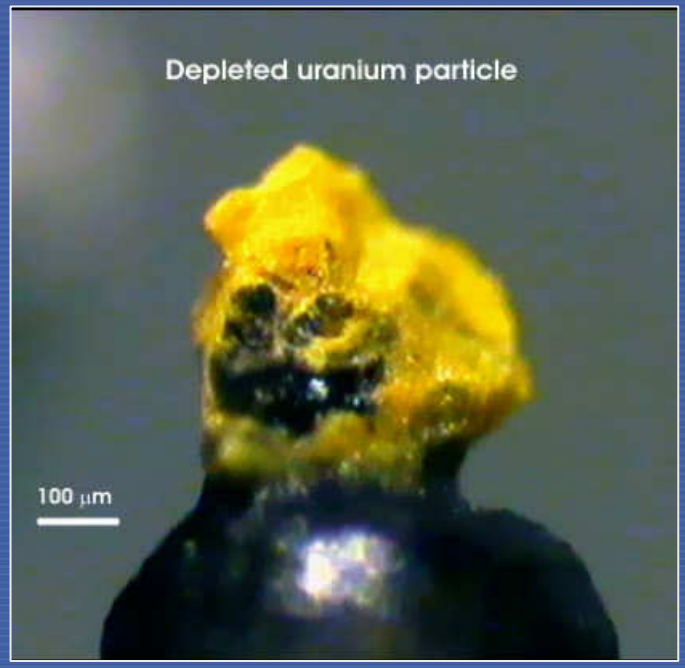

Reconstructed volumetric model (left) of a DU grain (right) obtained in absorption mode

IAEA

4. Depleted Uranium Particle

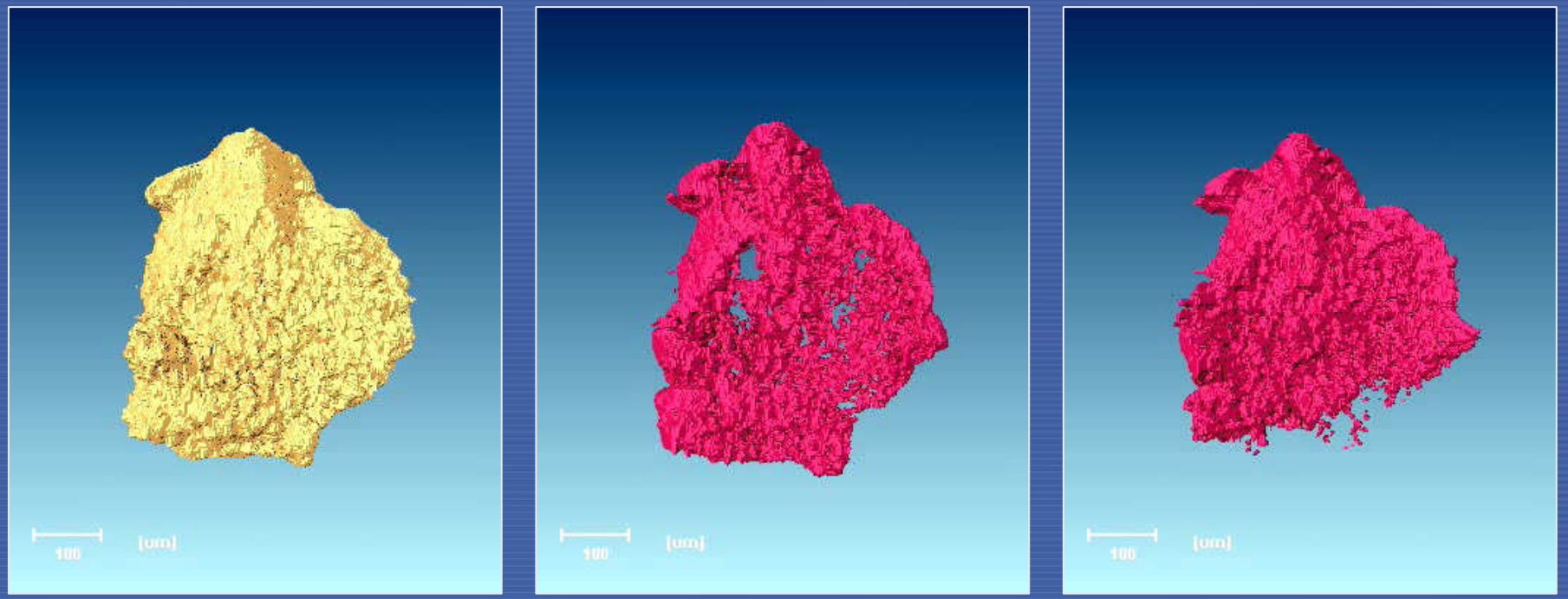

Reconstructed volumetric models of a DU grain (left to right): absorption, U-La not corrected for absorption and U-La corrected

5. Depth profiling of element distribution with confocal setup

a) – g) distributions of the intensities of scatter peaks, K-Ka, Ca-Ka, Mn-Ka, Fe-Ka, Zn-Ka, and U-La obtained from cross-sectional confocal X-ray fluorescence scan through the root tip. Scan parameters: step size dx = 22.124 μm, dy = 20.000 μm, scan size 19x21 pixels, spectra acquisition time per pixel = 500s for "live pixels", 1 s for others, spatial resolution of the confocal setup FWHM = 60 μm, Mo-anode X-ray tube operated at 45kV/40 mA; h) cumulative X-ray spectrum (sum of all individual pixel spectra) collected during the confocal scan; i) photograph of the indian mustard root.

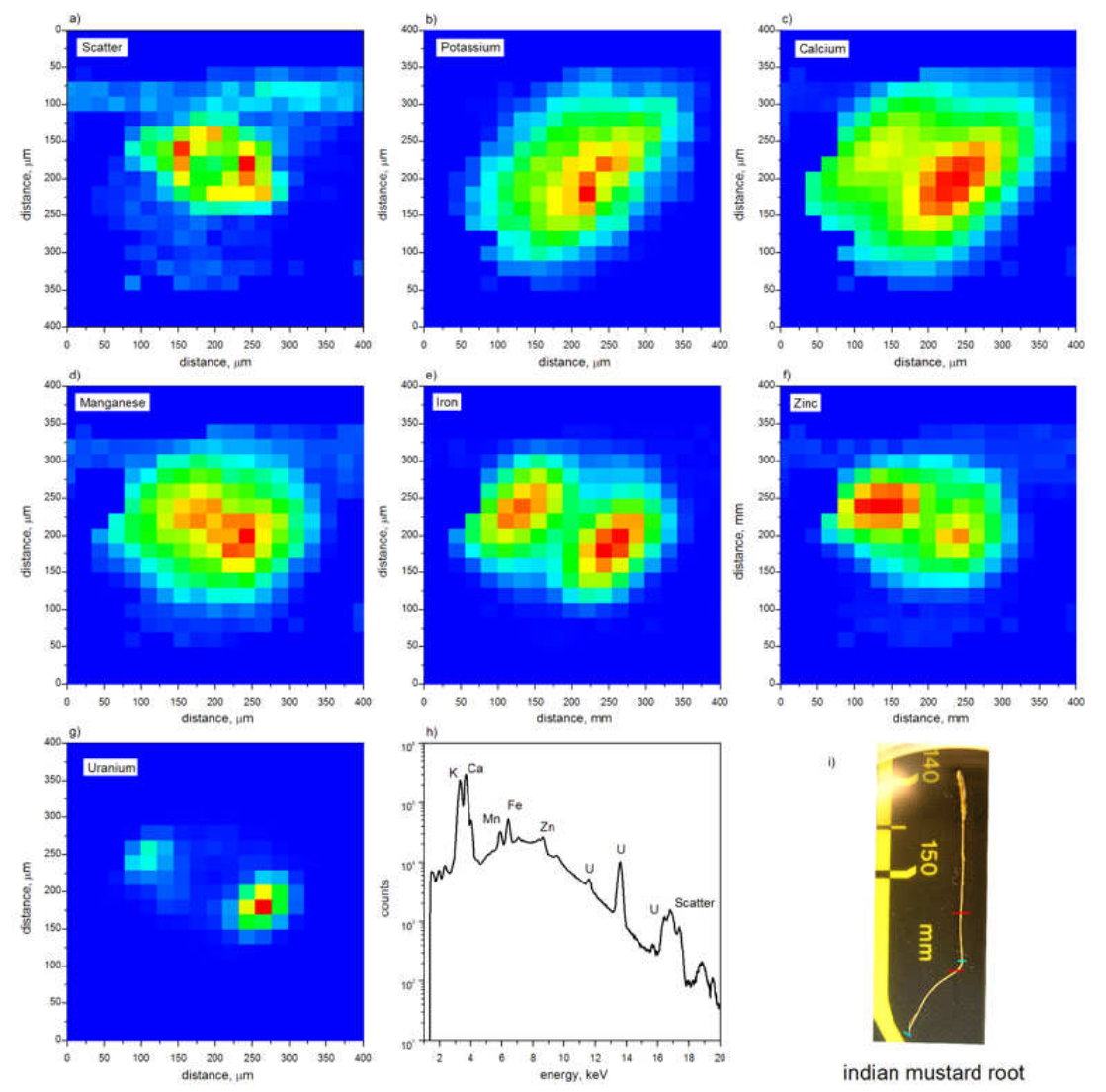

5. Distribution of elements in human bone obtained by confocal scanning

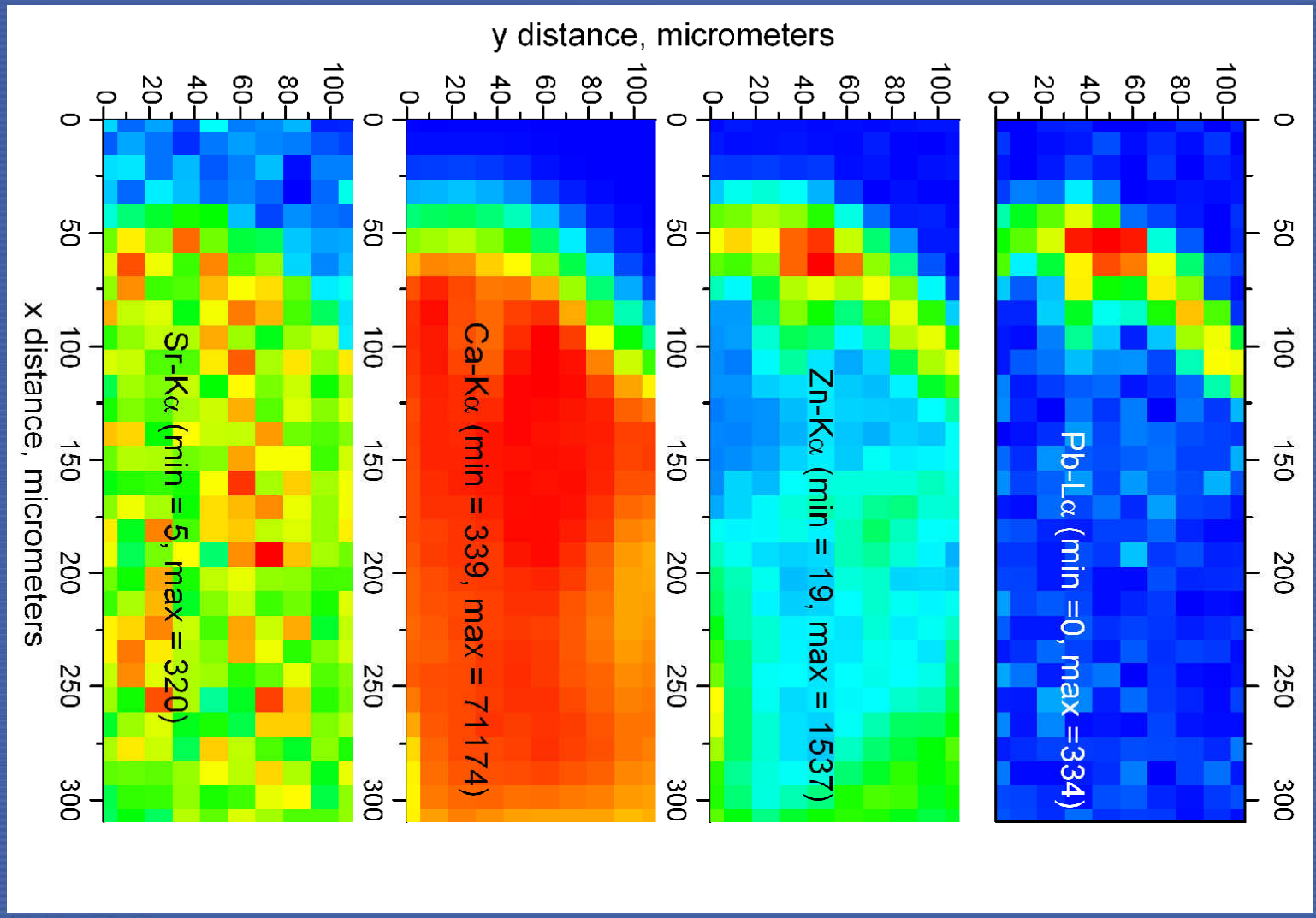

5. Fe-rich plaque covering rice root

red – iron

yellow – potassium

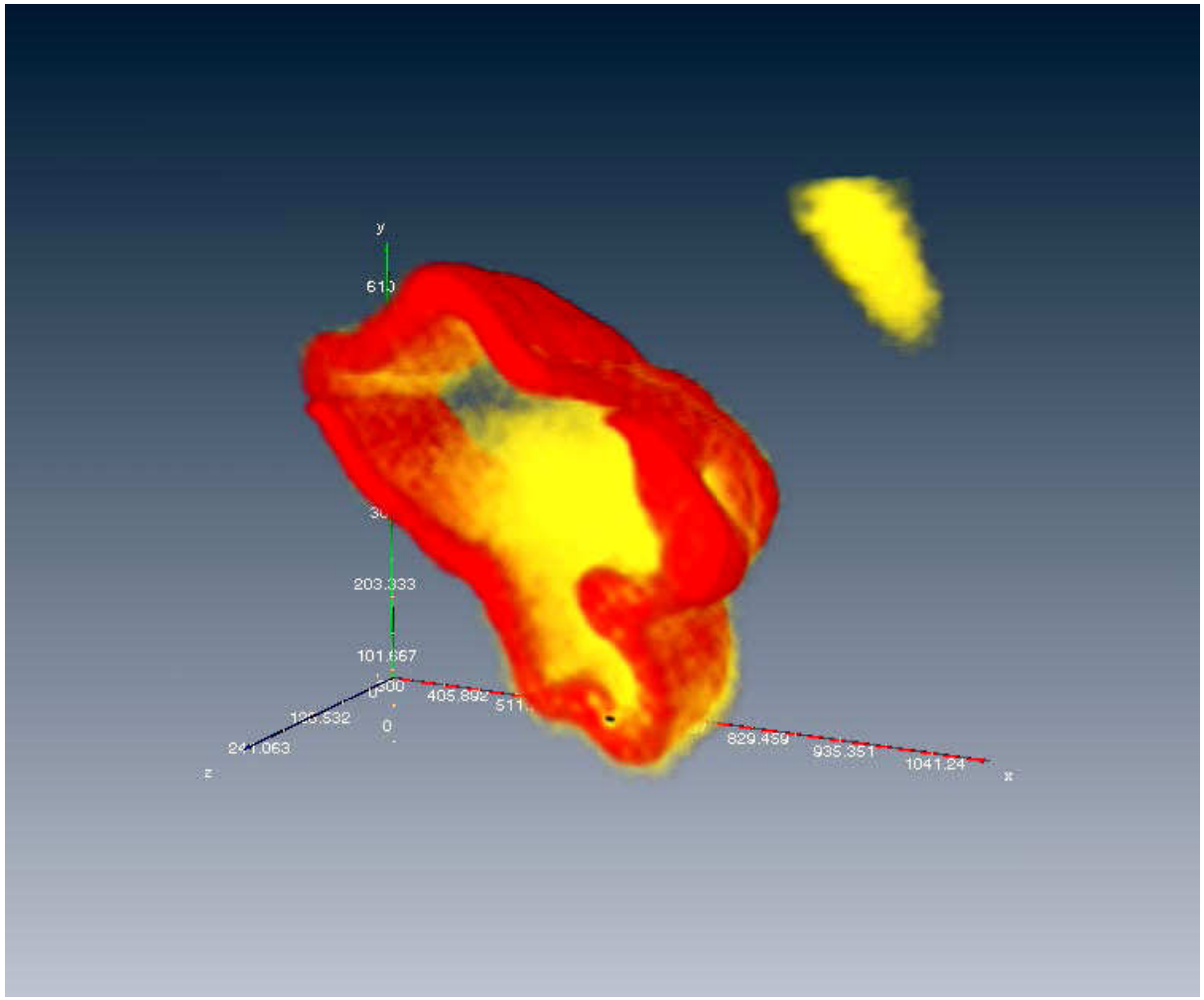

IAEA

6. Sample preparation procedures

For micro-analytical techniques (micro XRF and micro-tomography)

- Individual particles
- Biological materials

6. Individual Particles

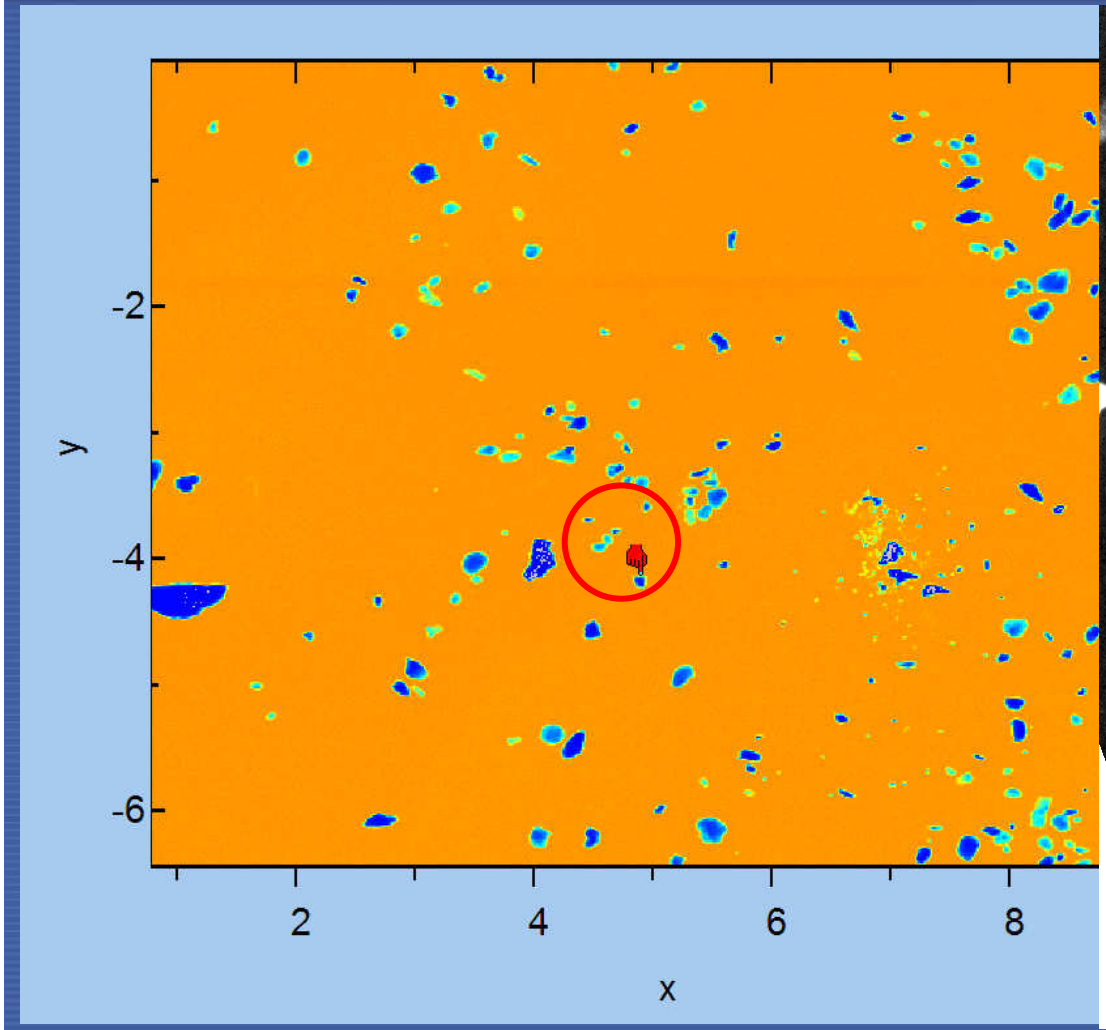

6. Individual Particles

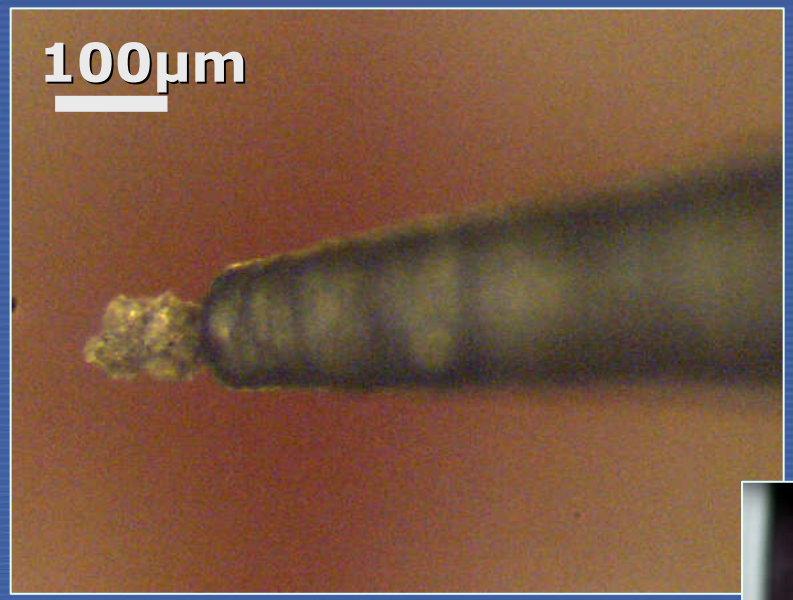

DU particle from a contaminated soil, loaded on a sharpened graphite needle

Loading the needle with a selected POI in the µ-manipulation system

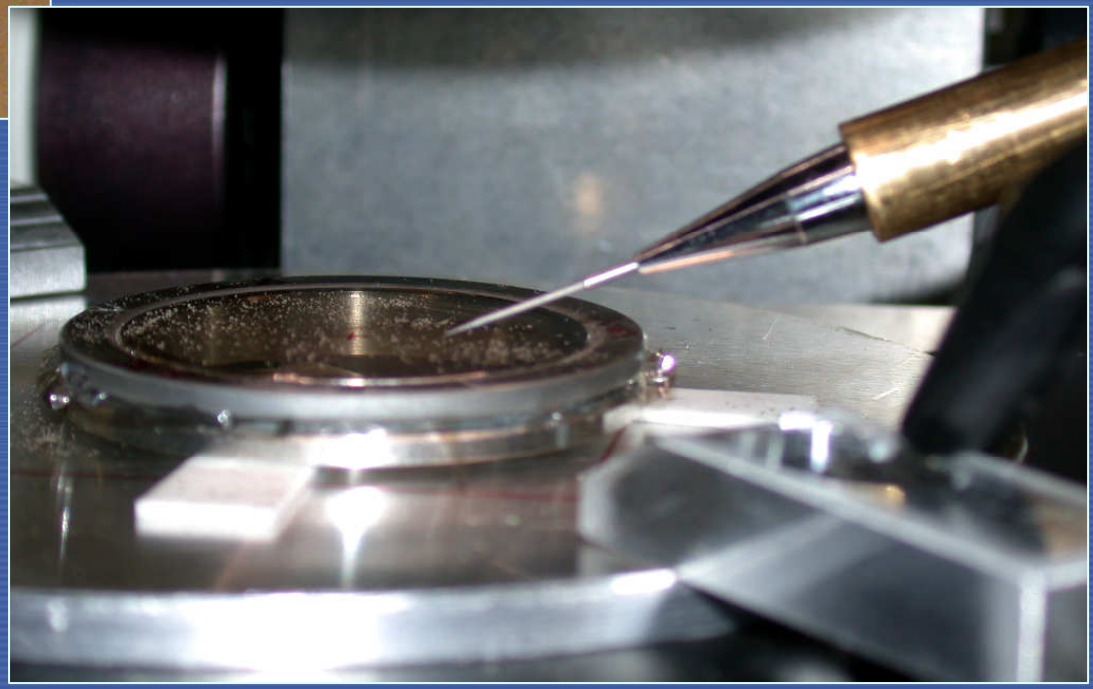

IAEA

6. Biological Materials

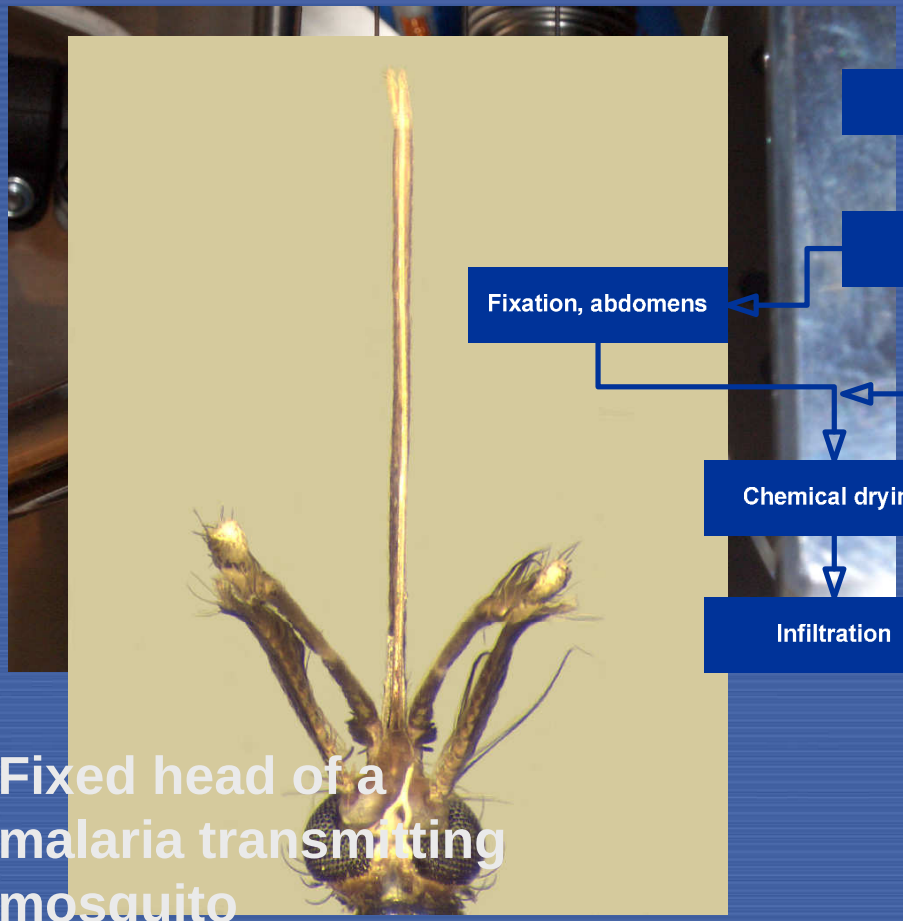

Fixed head of a malaria transmitting mosquito

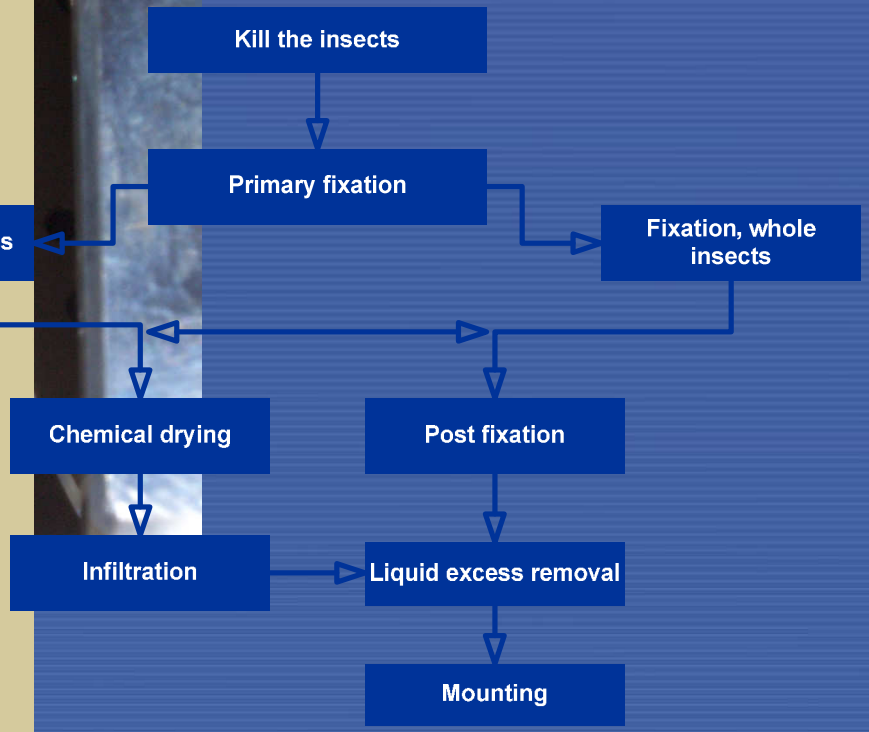

7. Micro-beam X-ray spectrometer installation at the ANKA synchrotron Fluo-Topo beamline

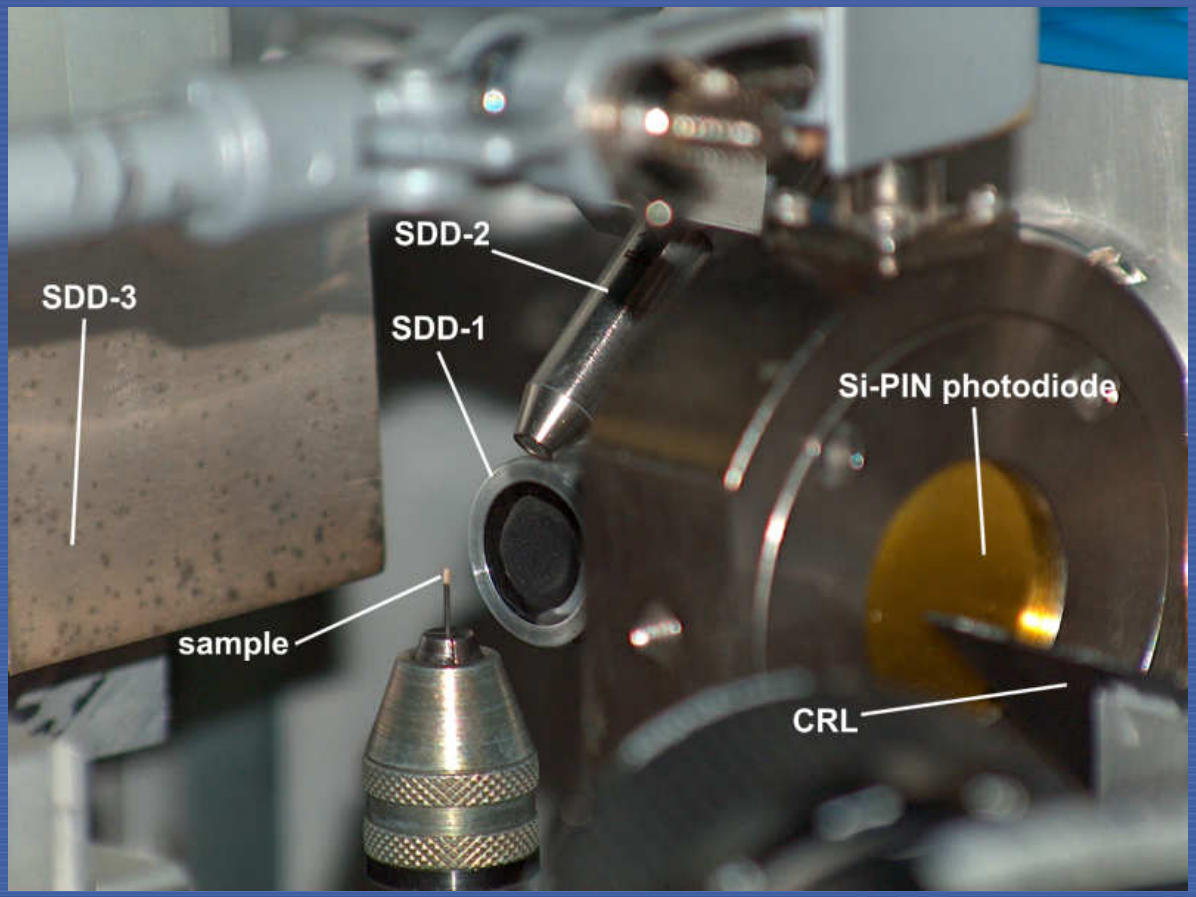

The IAEA micro-beam X-ray scanning spectrometer setup installed at the ANKA Fluo-Topo beamline, FZK Research Centre, Karlsruhe, Germany.

IAEA

7. Angstrom Quelle Karlshure (ANKA)

The IAEA set-up at the synchrotron beamline

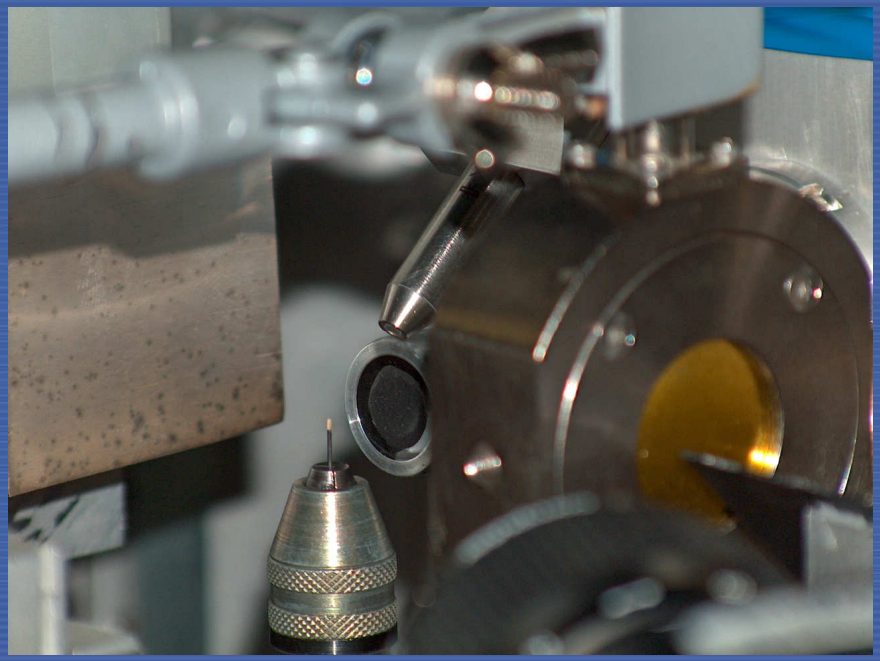

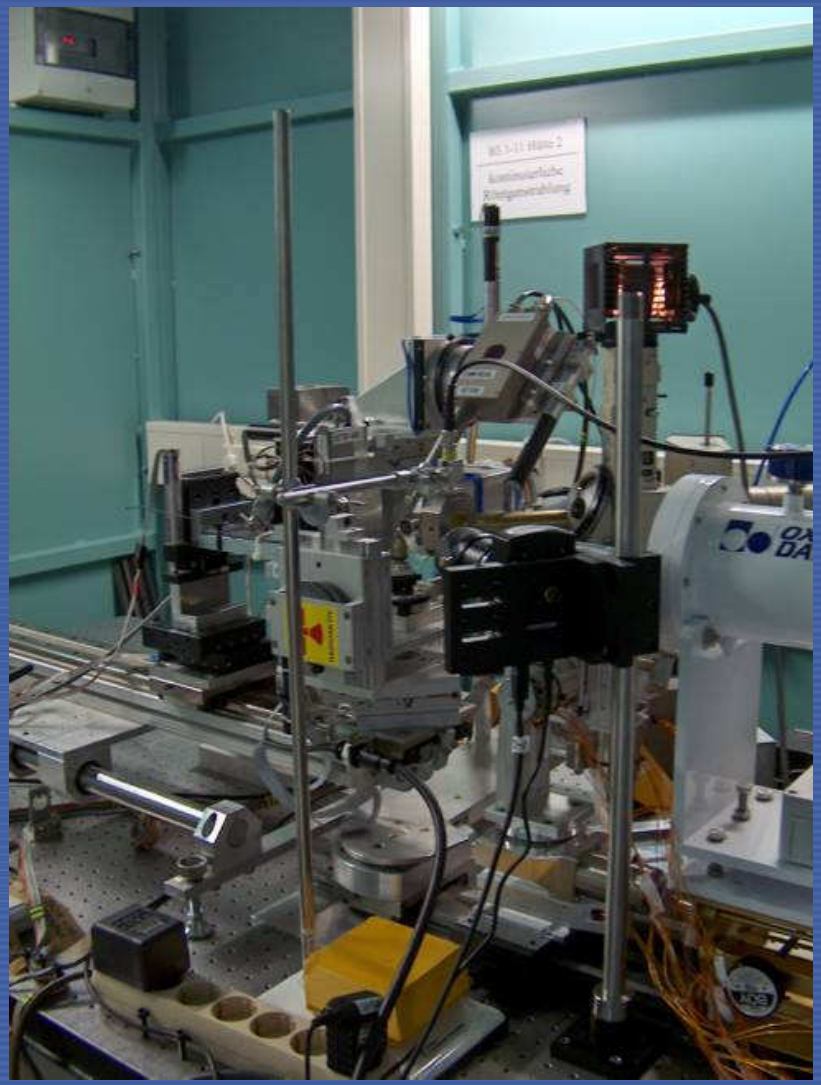

7. X-ray fluorescence micro tomography

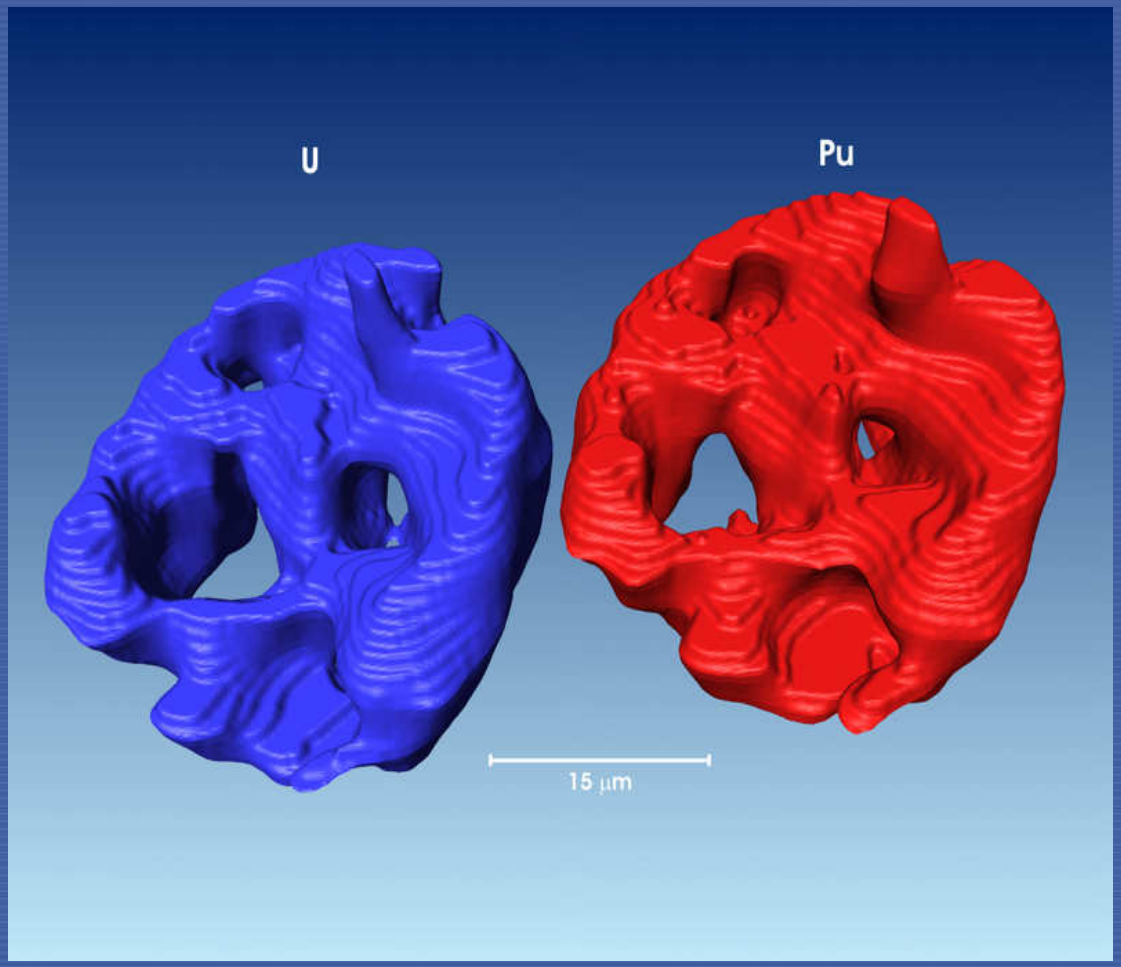

3D reconstruction of the spatial distributions of uranium and plutonium in a U/Pu-rich particle.

7. Pu/U-rich particles – X-ray tomography

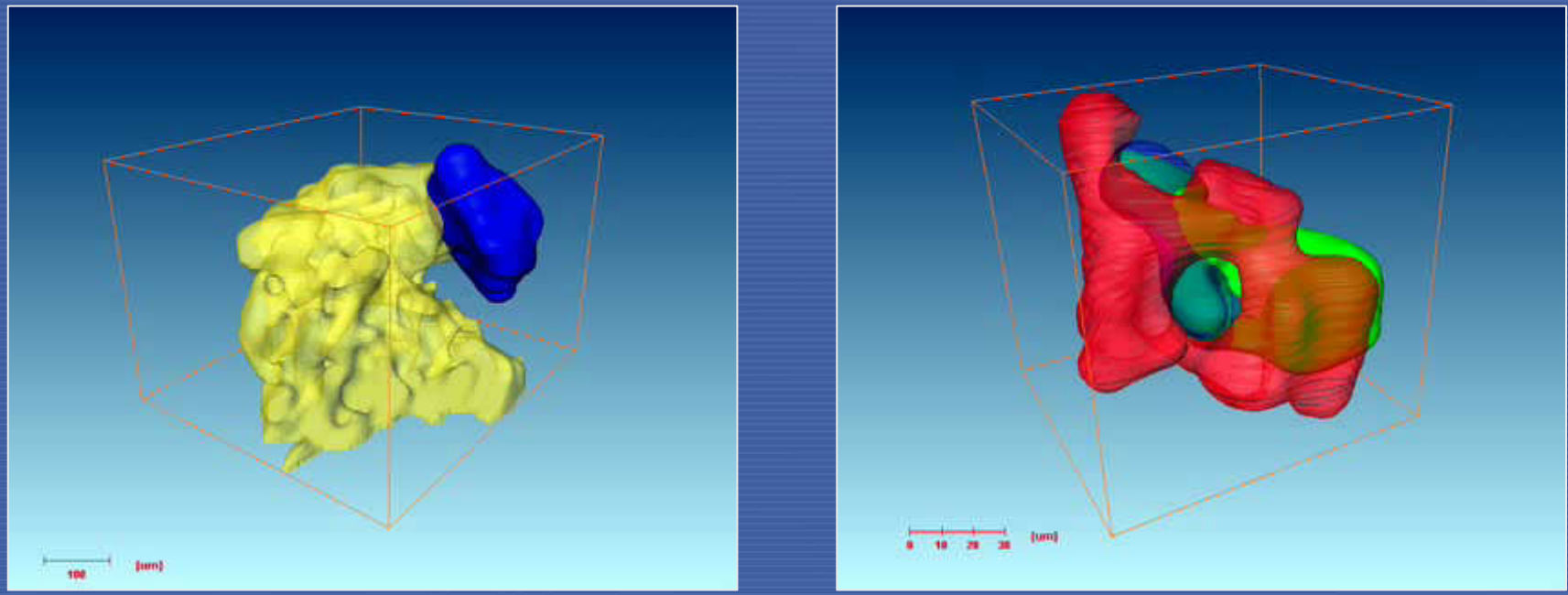

Reconstructed volumetric distributions of elements in individual “hot particles”: left - plutonium rich particle (blue) attached to a coral matrix (yellow) and right – a U/Pu rich particle (green/blue) embedded in sediment matrix (red)

7. X-ray fluorescence micro tomography

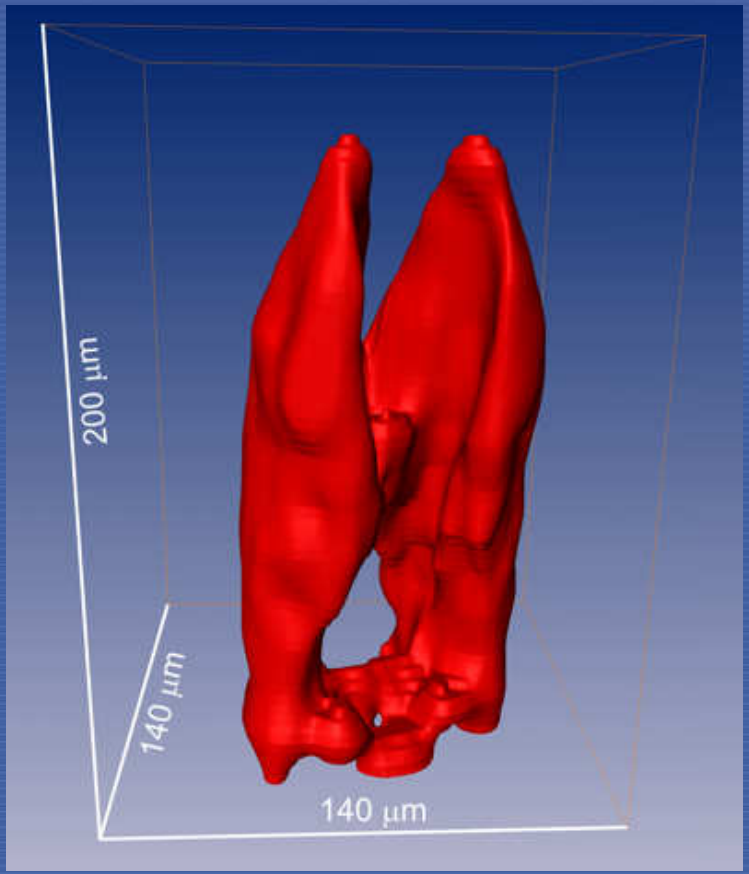

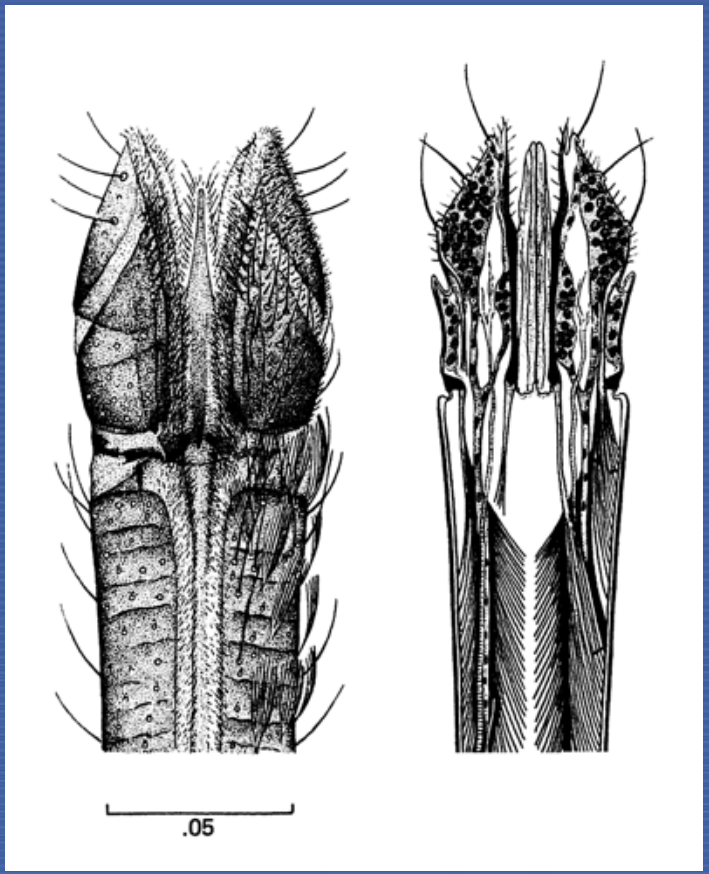

Left: tomographic reconstruction of the last segments of the proboscis of a female mosquito (Anopheles); right: anatomical drawing of Aedes Aegypti, adopted from Jobling, Boris and David James Lewis, Anatomical Drawings of biting flies, British Museum of Natural History, London, in association with the Wellcome Trust, 1987. The filtered backprojection algorithm was used to reconstruct the uranium-fixed proboscis of a female mosquito.

7. X-ray phase-contrast enhanced micro tomography

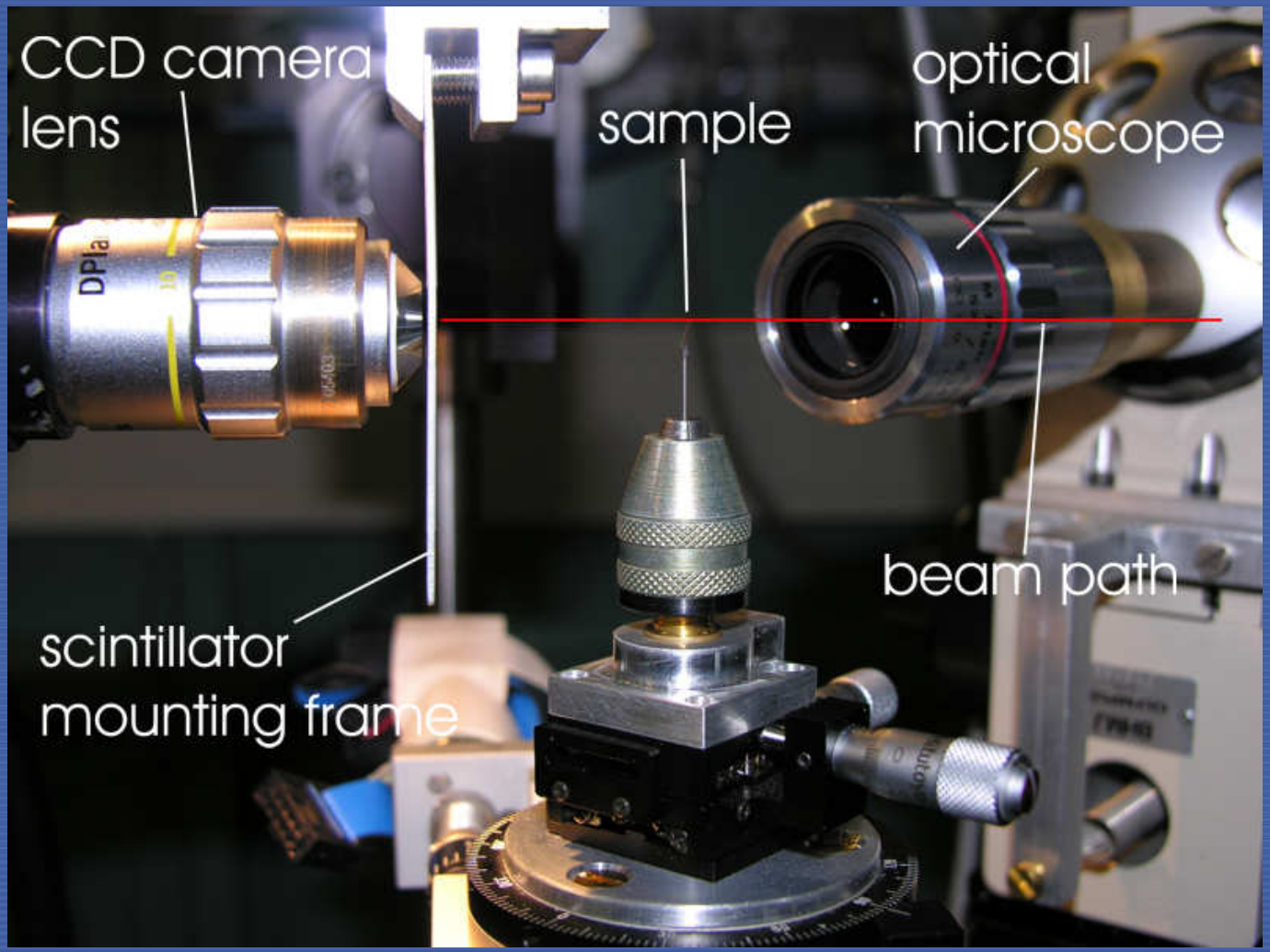

Experimental setup established at the ANKA synchrotron Fluo-Top beam line for investigating the morphology of malaria transmitting mosquitoes

7. X-ray phase-contrast enhanced micro tomography

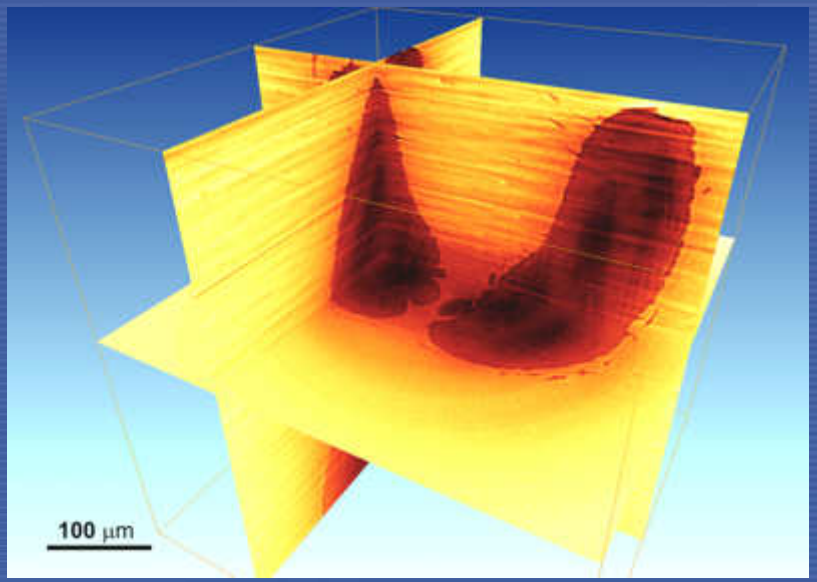

Left: single X-ray phase-contrast enhanced projection image of an abdomen of irradiated male mosquito; right: reconstructed volumetric cross-section through the mosquito abdomen

7. X-ray phase-contrast enhanced micro tomography

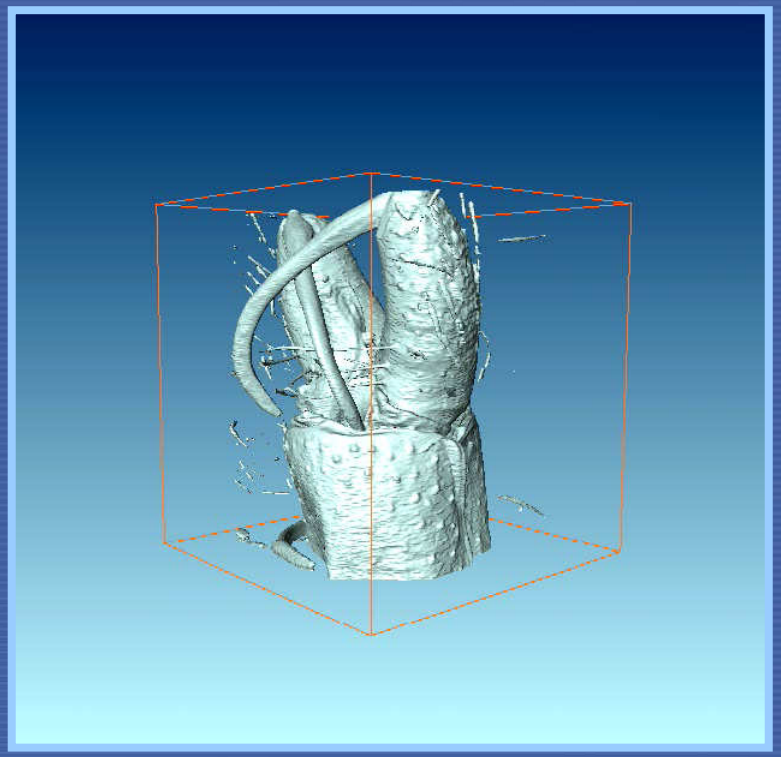

Left: single X-ray phase-contrast enhanced projection image of an abdomen of irradiated male mosquito; right: reconstructed volumetric model through the mosquito abdomen

IAEA

7. Phase-contrast X-ray imaging of live specimens

8. Training

Model XRF laboratory for basic and advanced training

- Training to develop practical skills
- Develop analytical procedures for special applications in IAEA MSs
- Research & development
- QA/QC procedures incl. uncertainty budget

9. Summary and conclusions

- **Integration** of R&D with training and direct analytical services to IAEA MSs
- **Extension** of applicability range and **improvement** in analytical performance of XRF are major concern
- Emphasis on **versatility** of XRF (important for XRF labs in developing countries)
- Emphasis on **usefulness** of the results for XRF laboratories

9. Summary and conclusions

- X-ray tube based micro-analytical techniques are well suited for characterization of minute samples, and heterogeneous objects.
- Quantitative analysis is possible but more difficult as compared to the analysis of bulk samples.
- When combined with synchrotron radiation very low amount of substance can be detected, coherent beam allows performing phase-contrast imaging of weakly absorbing objects, e.g. tissue, biomedical samples.

Acknowledgements

The results presented were obtained with collaboration of:

- D.Wegrzynek, E. Chinea-Cano, S. Bamford, C. A. Malcolm and M. Helinski, IAEA Laboratories Seibersdorf
- P. Wobrauschek, C. Streli, N. Zoeger, Vienna University of Technology, Atominstitut, Austria
- M. Eriksson, M. Betti, S. Toeroek, European Commission Joint Research Center, Institute for Transuranium Elements, Karlsruhe , Germany
- R. Simon, S. Staub, T. Weitkamp, A. Rack, Forschungszentrum Karlsruhe GmbH, Institute for Synchrotron Radiation, Eggenstein-Leopoldshafen, Germany

THANK YOU

E-mail: A.Markowicz@iaea.org